BOND BEHAVIOR OF GRADE 100 ASTM A 1035 REINFORCING STEEL IN BEAM-SPLICE SPECIMENS

By
Michael Briggs
Shelby Miller
David Darwin
JoAnn Browning

A Report on Research Sponsored by

MMFX TECHNOLOGIES CORPORATION

Structural Engineering and Engineering Materials
SL Report 07-1
August 2007 (Revised October 2007)

THE UNIVERSITY OF KANSAS CENTER FOR RESEARCH, INC.
2385 Irving Hill Road, Lawrence, Kansas 66045-7563

Bond Behavior of Grade 100 ASTM A 1035 Reinforcing Steel in Beam-Splice Specimens

By

Michael Briggs
Shelby Miller
David Darwin
JoAnn Browning

A Report on Research Sponsored by
MMFX Technologies Corporation

Structural Engineering and Engineering Materials
SL Report 07-01

THE UNIVERSITY OF KANSAS CENTER FOR RESEARCH, INC.
LAWRENCE, KANSAS

August 2007 (Revised October 2007)

Executive Summary

The bond behavior of Grade 100 ASTM A 1035 deformed steel reinforcing bars manufactured by MMFX Technologies Corp., operating at stresses from 80 to 140 ksi, is evaluated. The reinforcement is tested using beam-splice specimens designed to investigate factors known to influence bond behavior, including splice length, bar size, concrete cover, concrete compressive strength, and transverse reinforcement. The tests were performed as part of a joint bond research program conducted at the University of Kansas (KU), North Carolina State University (NCSU), and the University of Texas at Austin (UT). This report describes the tests performed at KU and summarizes the data from the three schools.

Of 69 specimens tested, 64 failed in bond in the splice region. Lap splices developed bar stresses between 68 and 155 ksi prior to failure. The use of confining transverse reinforcement significantly increased splice strength and deformation capacity of the beam specimens.

The development length equation proposed in ACI 408R-03 is an accurate predictor for the beam-splice specimens, with a coefficient of variation of test/prediction ratios of 0.11 for splices without confining transverse reinforcement, and 0.10 for those with confining transverse reinforcement. The development length equation in ACI 318-05 exhibited more scatter with respect to the test data than the ACI 408R-03 equation and significantly over predicted bar stress in splices without confining transverse reinforcement, indicating that it cannot be used for development length and splice design with Grade 100 reinforcing steel. A development length equation proposed by NCSU as part of this study provides an accurate representation of strength for splices without confining transverse reinforcement.

Acknowledgements

This study was funded by MMFX Technologies Corporation. Additional support was provided by Dayton Superior Corporation, W. R. Grace & Co., LRM Industries, Builder's Steel, the Kansas Department of Transportation, and the University of Kansas Department of Civil, Environmental & Architectural Engineering.

Table of Contents

List of Tables

List of Figures

1.0 Introduction

Bond strength is an important factor in the behavior of reinforced concrete members. The recent development of high-strength deformed reinforcing steel, such as commercially-available Micro-composite Multi-structural Formable (MMFX) steel, poses new questions regarding the behavior of members containing reinforcement operating at stresses well above those previously studied.

Empirical design and analysis equations used to calculate bond strength, such as those found in ACI 318-05 and ACI 408R-03, were calibrated using Grades 40, 60 and 75 steels. The failure stresses in most of these tests were well below 100 ksi, and the bond behavior of deformed steel reinforcing bars operating at stresses greater than 100 ksi are neither well documented nor well represented in the equations for bond strength prediction.

The objective of this research program is to evaluate the bond behavior of Grade 100 ASTM A 1035 deformed steel reinforcing bars, manufactured by MMFX Technologies Corporation, operating at stresses from 80 to 140 ksi. To accomplish this, a series of splice tests were performed to determine the bond behavior of the steel at high stresses. Beam-splice specimens were designed to investigate factors known to influence bond behavior, including splice length, bar size, concrete cover, concrete compressive strength, and transverse reinforcement.

The analysis in this report will focus on data collected from the three universities participating in the joint bond research program – the University of Kansas (KU), North Carolina State University (NCSU), and the University of Texas at Austin (UT). The fabrication and testing procedures described in this report are provided only for the tests performed at KU, as are certain test results. Detailed test results for the KU specimens are presented in Appendix B.

2.0 Research Program and Test Specimens

2.1 General

2.1.1 Overview

As recommended by ACI Committee 408, beam-splice specimens were used to study the bond behavior of the reinforcing steel. The specimens tested at the University of Kansas were designed to achieve a stress in the tension steel of 150 ksi at flexural failure. Splice lengths, confining transverse reinforcement, and concrete cover dimensions were selected to achieve a bond failure within the splice at stress levels in the tension steel of 80, 100, 120, or 140 ksi based on bond strength prediction equations in ACI 408R-03.

Of the sixty-nine beams tested in the study, twenty-two specimens were tested at KU with the following parameters:

No. 5 bars:

- ¾ in. and $2d_b$ cover
- 18, 25, 32, and 43 in. splice lengths, ℓ_s
- 5000 psi target concrete compressive strength, f'_c
- All splices unconfined

No. 8 bars:

- 1 ½ in. and 2 ½ in. cover
- 27, 36, 47, and 63 in. splice lengths, ℓ_s
- 5000 and 8000 psi target concrete compressive strength, f'_c
- 0, 2, 4, 5, and 8 No. 4 bar stirrups confining the splice

No. 11 bars:

- 2 in. cover
- 58 and 79 in. splice lengths, ℓ_s
- 8000 psi target concrete compressive strength, f'_c
- 0, 4, and 9 No. 4 bar stirrups confining the splice

where d_b is the nominal bar diameter.

Test specimens are identified using a notation system common to the three universities. The notation designates the size of the spliced bars, the concrete compressive strength in ksi, the bar stress level for splices without confining steel, the level of confinement, and the concrete clear cover. Beams were designed in groupings of six with identical cover, dimensions, and span lengths. The beams in a series differ in terms of splice length (two lengths were used) and level of confinement (three levels were used). Beams are identified as shown in Figure 2.1 and described in Section 2.1.2.

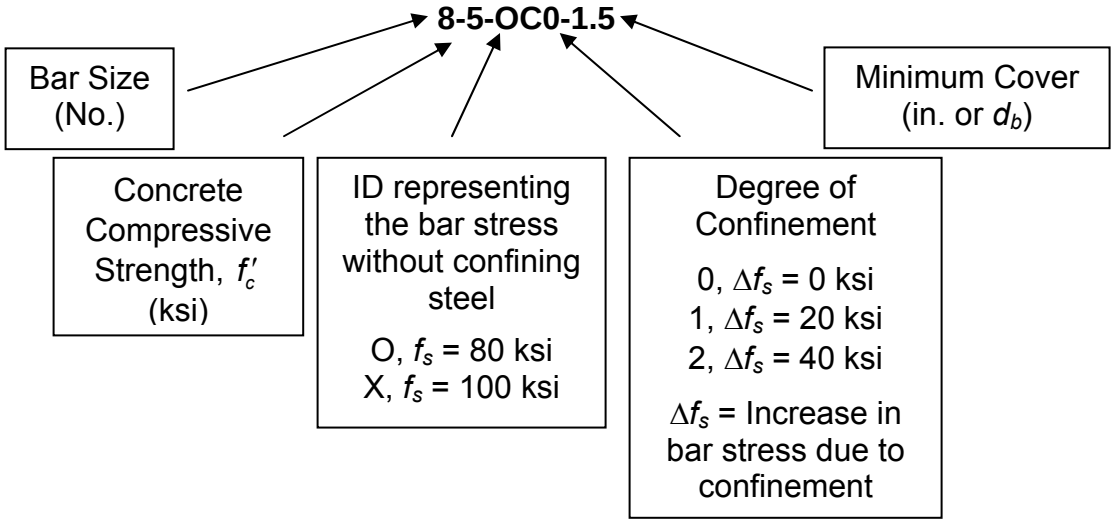

Figure 2.1 – Sample notation for a beam-splice test specimen

2.1.2 Collective Test Program

Each school was assigned principal responsibility for three series of specimens plus two sets of two beams from series for which another university had prime responsibility. Table 2.1 summarizes the test program. Duplicate beams are shown in bold. The test specimens include those from the original program of sixty-six beams plus three extra specimens tested at UT for the purpose of evaluating the effect of concrete compressive strength. These specimens are duplicates of specimen 8-8-OC_-1.5 at 0, 1 and 2 levels of confinement, but were instead cast with 5 ksi concrete. To avoid confusion with specimens already titled 8-5-OC_-1.5, which have a different splice length, these duplicates are designated as 8-5-SC_-1.5, in which 'S' denotes a "special" design bar stress without confining steel.

Table 2.1 – Matrix of all specimens tested at KU, NCSU, and UT

f'_c (ksi)	d_b (No.)	Cover (in.)	KU O**	KU X**	NCSU O	NCSU X	UT* O	UT* X
5	5	3/4	**0**	**0**			**0**	**0**
		$2d_b$	**0**	**0**			**0**	**0**
		$3d_b$					0	0
	8	1.5	**0**,1,**2**	**0**,1,**2**			**0**,**2**	**0**,**2**
		2.5			0,1,2	0,1,2		
	11	2			0,1,2	0,1,2		
		3					0,1,2	0,1,2
8	8	1.5			**0**,**2**	**0**,**2**	**0**,1,**2**	**0**,1,**2**
		2.5	0,1,2	0,1,2				
	11	2	0,1,2	0,1,2				
		3			0,1,2	0,1,2		
Total Specimens			22		22		22	

Confinement Levels

*Does not show UT specimens 8-5-SC0-1.5, 8-5-SC1-1.5, and 8-5-SC2-1.5

**ID representing the bar stress without confining transverse steel

Five series of specimens were tested at KU, as shown in Table 2.2. Series 1 and 2 are duplicates of beams tested at UT, while Series 3, 4, and 5 are complete sets of six. The series are split into groups according to splice length; 'A' denotes the shorter of the two splice lengths (and lower bar stress at splice failure), while 'B' is the longer (with the higher bar stress at splice failure).

Table 2.2 – Design details of beam-splice specimens tested at KU

Series	Group	Specimen	Bar Size	Nominal f'_c	Minimum Design Cover	Nominal Section, b x h	Splice Length	Design Stress
			(No.)	(ksi)	(in.)	(in. x in.)	(in.)	(ksi)
1	A	**5-5-OC0-3/4**	5	5	0.75	14 x 20	32	80
	B	**5-5-XC0-3/4**					43	100
2	A	**5-5-OC0-2d_b**			1.25	35 x 10	18	80
	B	**5-5-XC0-2d_b**					25	100
3	A	**8-5-OC0-1.5**	8	5	1.5	14 x 30	47	80
		8-5-OC1-1.5						100
		8-5-0C2-1.5						120
	B	**8-5-XC0-1.5**					63	100
		8-5-XC1-1.5						120
		8-5-XC2-1.5*						140
4	A	**8-8-OC0-2.5**		8	2.5	14 x 21	27	80
		8-8-OC1-2.5						100
		8-8-OC2-2.5						120
	B	**8-8-XC0-2.5**					36	100
		8-8-XC1-2.5						120
		8-8-XC2-2.5						140
5	A	**11-8-OC0-2**	11	8	2	24 x 26	58	80
		11-8-OC1-2						100
		11-8-OC2-2						120
	B	**11-8-XC0-2**					79	100
		11-8-XC1-2						120
		11-8-XC2-2**						140

*T-beam with b_f = 28 in. and h_f = 7 in.

**T-beam with b_f = 38 in. and h_f = 7 in.

2.2 Design of Test Specimens

The design methods described in this section were used for the specimens tested at KU, although the procedures were similar if not identical at all three universities. Table 2.3 summarizes the geometrical and reinforcement details of the twenty-two beam-splice specimens tested at KU.

Table 2.3 – Summary of flexural design details for KU specimens

Specimen		Design Beam Dimensions						Longitudinal Reinforcement				
Group	Designation	Support Spacing (ft)	Span, L (ft)	Width, b (in.)	Height, h (in.)	Effective Depth, d (in.)	Depth to A_s', d' (in.)	Bar Size (No.)	No. of Bars (ea.)	Area of Tension Steel, A_s ($in.^2$)	Area of Compr. Steel, A_s ($in.^2$)	Target Bar Stress, f_s (ksi)
1A	5-5-OC0-3/4	7	15	14	21*	18.94	1.81	5	4	1.76	1.76	80
1B	5-5-XC0-3/4	7	15	14	21*	18.94	1.81	5	4	1.76	1.76	100
2A	5-5-OC0-2d_b	7	15	35	10	8.44	1.75	5	4	1.76	0.80	80
2B	5-5-XC0-2d_b	7	15	35	10	8.44	1.75	5	4	1.76	0.80	100
3A	8-5-OC0-1.5	10	21	14	30	28.00	1.75	8	2	1.58	0.40	80
	8-5-OC1-1.5	10	21	14	30	28.00	1.75	8	2	1.58	0.40	100
	8-5-OC2-1.5	10	21	14	30	28.00	1.75	8	2	1.58	0.40	120
3B	8-5-XC0-1.5	10	21	14	30	28.00	1.75	8	2	1.58	0.40	100
	8-5-XC1-1.5	10	21	14	30	28.00	1.75	8	2	1.58	0.40	120
	8-5-XC2-1.5	10	21	28**	30	28.00	2.00	8	2	1.58	3.16	140
4A	8-8-OC0-2.5	10	21	14	21	18.00	2.00	8	2	1.58	1.58	80
	8-8-OC1-2.5	10	21	14	21	18.00	2.00	8	2	1.58	1.58	100
	8-8-OC2-2.5	10	21	14	21	18.00	2.00	8	2	1.58	1.58	120
4B	8-8-XC0-2.5	10	21	14	21	18.00	2.00	8	2	1.58	1.58	100
	8-8-XC1-2.5	10	21	14	21	18.00	2.00	8	2	1.58	1.58	120
	8-8-XC2-2.5	10	21	14	21	18.00	2.00	8	2	1.58	1.58	140
5A	11-8-OC0-2	11	24	24	26	23.50	1.75	11	2	3.12	0.40	80
	11-8-OC1-2	11	24	24	26	23.50	1.75	11	2	3.12	0.40	100
	11-8-OC2-2	11	24	24	26	23.50	1.75	11	2	3.12	0.40	120
5B	11-8-XC0-2	11	24	24	26	23.50	1.75	11	2	3.12	0.40	100
	11-8-XC1-2	11	24	24	26	23.50	1.75	11	2	3.12	0.40	120
	11-8-XC2-2	11	24	38**	26	23.50	1.97	11	2	3.12	3.56	140

*Height of Series 1 specimens was 20 in. for the middle 6 ft. of the beam.

**T-beam flange width, b_f. General beam width b identical to other beams in group.

2.2.1 Flexural Design

The test specimens were designed as typical rectangular reinforced concrete beams with nominal flexural capacities based upon maximum tensile bar stresses of 150 ksi. The beams were subjected to four-point loading to provide a constant moment region in the middle portion of the member, the location of the splice. A strength design approach was used for flexural capacity, using the Whitney stress block to represent concrete in compression. Values of β_1 from ACI 318-05 were used based upon the nominal concrete compressive strength.

Tension Steel

The longitudinal tension reinforcement was Grade 100 ASTM A 1035 reinforcing steel manufactured by MMFX Technologies Corp. The stress-strain relationship used for flexural design with MMFX steel was that proposed by Dawood et. al. (2004), shown in Eq. (2.1).

$$f_s = 165(1 - e^{-185\varepsilon_s}) \tag{2.1}$$

where:

f_s = stress in the steel, ksi

ε_s = strain in the steel

The specimens in Series 1 and 2 were designed to simulate slabs, and contained four No. 5 bars as tension reinforcement. Specimens in Series 3 and 4 contained two No. 8 bars, while those in Series 5 used two No. 11 bars as primary reinforcement.

Compression Steel

All specimens contained longitudinal bars in the compression region to anchor the upper corners of the stirrups used for shear and the transverse confining reinforcement. The specimens in Series 1 and 4 were designed using compression steel to provide adequate flexural capacity for the beam, while all other designs ignored the presence of top steel because the bars were small and not required to provide flexural strength. Specimens in Series 1 contained four No. 5 bars, whereas specimens in Series 4 contained two No. 8 bars. Specimens in Series 2 used four No. 4 bars to anchor the corners of the stirrups, while specimens in both Series 3 and 5 used two No. 4 bars. All compression steel consisted of standard Grade 60 ASTM A 615 bars and was assumed to follow a bi-linear stress-strain curve as described by Eq. (2.2).

$$f_s = 29000 \times \varepsilon_s \leq 60 \text{ ksi} \tag{2.2}$$

Concrete

Target concrete compressive strengths of 5 and 8 ksi were selected to represent concrete strengths found in actual construction because mixes with specified strengths of 4 and 6.5 ksi often reach 5 and 8 ksi, respectively. All specimens were cast with normalweight, non-air-entrained concrete consisting of Ash Grove Type I/II portland cement, water, Kansas River sand, and crushed limestone coarse aggregate with a maximum aggregate size of ¾ in. High-range water reducing admixtures (HRWRAs) were used in all 8 ksi mixes and as needed in 5 ksi mixes to meet workability targets. No pozzolanic admixtures were used. Full mix design details are presented in Tables A.1, A.2, and A.3 in Appendix A.

T-beam Specimens

Early in the testing program, specimen 8-5-XC2-1.5 failed in flexure in the compression region near the support. As a result, both that specimen and 11-8-XC2-2 were redesigned as T-beams with larger amounts of compression steel to increase their flexural capacity and avoid flexural failures in specimens with predicted bar forces at splice failure of 140 ksi. Specimen 8-8-XC2-2.5, the other beam tested at KU with a predicted bar stress of 140 ksi, had already been cast and failed in bond in the splice region and therefore did not have to be redesigned.

The flanges on both specimens were 14 in. wider than the original web width and 7 in. deep. Additional compression reinforcement, consisting of four No. 8 bars, was used for both beams. All other properties of the beams remained unchanged.

2.2.2 Shear Design

Shear reinforcement for the portions of the beams outside of the central constant moment region was designed in accordance with procedures outlined in ACI 318-05. The spacing of closed stirrups s_2 varied between 4 and 5 in. (Table 2.4). Series 1 through 4 used No. 4 closed stirrups as shear reinforcement, while Series 5 used No. 5 stirrups. The closed stirrups were made with Grade 60 ASTM A 615 steel and fabricated with 135º hooks at one corner. The majority of the stirrups used in the testing program and all of the stirrups used in specimens in Series 1 and 5 were bent at a fabricating shop; some of the stirrups used in Series 2, 3, and 4 were fabricated at KU.

2.2.3 Splice Design

Splice Length and Confinement

Test specimens were designed with lap splices centered at the midspan of the beam. Two splice lengths ℓ_s were selected for each series that, according to ACI 408R-03, would result in bond failure at bar stresses of 80 and 100 ksi if the splices were not confined by transverse reinforcement. These specimens were designated as "OC_" or "XC_", with "O" denoting the shorter splice length, and "X" the longer. Stirrups provided two levels of confinement, "_C1" and "_C2", designed to increase the bar stress at failure for each splice length by 20 or 40 ksi, respectively. The nominal center-to-center spacing between transverse reinforcement over the length of the splice s_1 is listed in Table 2.4. The resulting nominal splice strengths are 80, 100, and 120 ksi for specimens OC0, OC1, and OC2, respectively, and 100, 120, and 140 ksi for specimens XC0, XC1, and XC2.

Concrete Cover

Test specimens containing No. 8 and No. 11 bars were designed to have equal amounts of concrete clear cover on the bottom c_b and sides c_{so} of the spliced bars to help ensure an equal likelihood of failure by bottom or side splitting. Series 4 (No. 8 bar) specimens had a clear spacing $2c_{si}$ equal to twice the concrete clear cover, while Series 3 (No. 8 bar) and 5 (No. 11 bar) had a clear spacing greater than two times the clear cover.

Specimens containing No. 5 bars, Series 1 and 2, were designed as slabs and thus had clear bar spacings that were greater than twice the bottom cover to simulate typical slab construction. Clear spacing remained twice the side cover. Figure 2.2 shows the typical cross-sectional layouts for all beam splice-specimens.

Table 2.4 – Splice and cover shear dimensions and shear reinforcement for KU beam-splice specimens

Specimen		Splice Design									Shear Reinforcement	
Group	Designation	Splice Length, l_s (in.)	Bottom cover, c_b (in.)	Outside cover, c_{so} (in.)	Half clear spacing c_{si} (in.)	No. 4 Stirrups (ea.)	C/C Tie Spacing, s_1 (in.)	Bar Size (No.)	No. of Bars (ea.)	Target Bar Stress, f_s (ksi)	Bar Size (No.)	C/C Spacing, s_2 (in.)
1A	5-5-OC0-3/4	32	0.75	1.13	1.13	--	--	5	4	80	4	4
1B	5-5-XC0-3/4	43	0.75	1.13	1.13	--	--	5	4	100	4	4
2A	5-5-OC0-2d_b	18	1.25	3.75	3.75	--	--	5	4	80	4	4
2B	5-5-XC0-2d_b	25	1.25	3.75	3.75	--	--	5	4	100	4	4
3A	8-5-OC0-1.5	47	1.5	1.5	3.5	--	---	8	2	80	4	4.5
	8-5-OC1-1.5	47	1.5	1.5	3.5	4	11 3/4	8	2	100	4	4.5
	8-5-OC2-1.5	47	1.5	1.5	3.5	8	5 7/8	8	2	120	4	4.5
3B	8-5-XC0-1.5	63	1.5	1.5	3.5	--	--	8	2	100	4	4.5
	8-5-XC1-1.5	63	1.5	1.5	3.5	4	15 3/4	8	2	120	4	4.5
	8-5-XC2-1.5	63	1.5	1.5	3.5	8	7 7/8	8	2	140	4	4.5
4A	8-8-OC0-2.5	27	2.5	2.5	2.5	--	--	8	2	80	4	5
	8-8-OC1-2.5	27	2.5	2.5	2.5	2	13 4/8	8	2	100	4	5
	8-8-OC2-2.5	27	2.5	2.5	2.5	5	5 3/8	8	2	120	4	5
4B	8-8-XC0-2.5	36	2.5	2.5	2.5	--	--	8	2	100	4	5
	8-8-XC1-2.5	36	2.5	2.5	2.5	2	18	8	2	120	4	5
	8-8-XC2-2.5	36	2.5	2.5	2.5	5	7 1/4	8	2	140	4	5
5A	11-8-OC0-2	58	2	2	7.18	--	--	11	2	80	5	4.5
	11-8-OC1-2	58	2	2	7.18	4	14 1/2	11	2	100	5	4.5
	11-8-OC2-2	58	2	2	7.18	9	6 1/2	11	2	120	5	4.5
5B	11-8-XC0-2	79	2	2	7.18	--	--	11	2	100	5	4.5
	11-8-XC1-2	79	2	2	7.18	4	19 3/4	11	2	120	5	4.5
	11-8-XC2-2	79	2	2	7.18	9	8 3/4	11	2	140	5	4.5

*Height of Series 1 specimens was 20 in. for the middle 6 ft. of the beam.

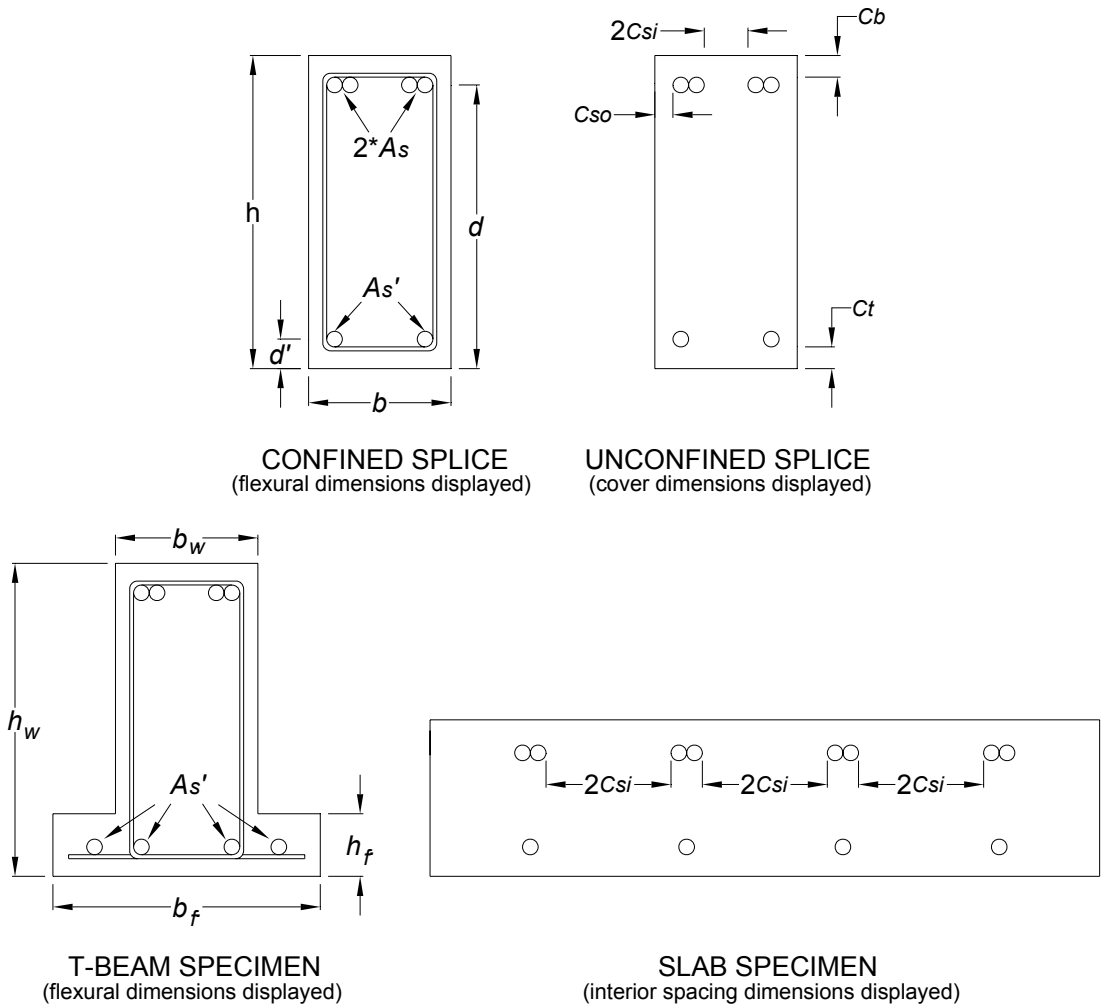

SECTION A-A

Figure 2.2 – Cross-sections of the splice region for all specimen types, as tested

2.2.4 Span Length

The nearly constant moment resulting from four-point loading eliminates the effects of shear forces in the splice region and therefore the need for shear reinforcement in the middle portion of the beam, allowing transverse reinforcement to be used solely as confinement for the splices rather than as shear reinforcement.

All specimens were designed so that the support spacing ensured a distance from either end of the splice to the central pin and roller supports equal to or greater than the effective depth of the beam *d*. The loading span lengths were selected to induce moments causing bar stresses of 150 ksi at moderate load levels. The span

lengths were selected in increments of 3 ft based on the available spacing of load points in KU's structural testing laboratory. The specimens were inverted for testing, as shown in Figures 2.2 and 2.3.

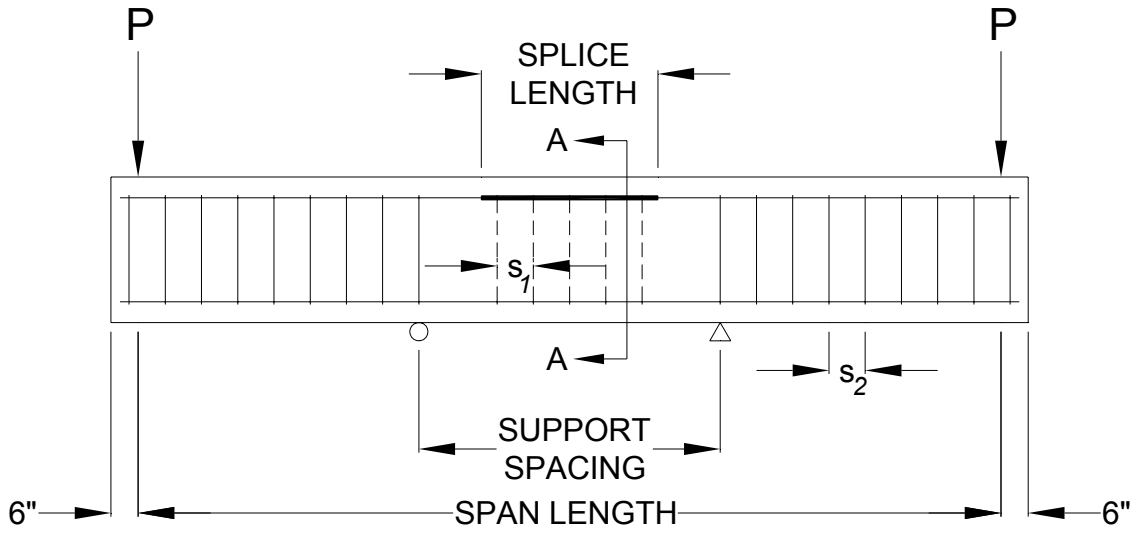

Figure 2.3 – Schematic showing elevation view of a test specimen

2.3 Construction Details

2.3.1 Reinforcement Cages

The beam specimens were constructed 1 ft longer than the design loading span to accommodate the loading apparatus. Longitudinal reinforcement was terminated 1 in. from the end of the specimen to allow for construction tolerances. Shear reinforcement was continued to the end of the longitudinal reinforcement.

Grade markings were allowed within the splice region. The grade markings did not interrupt the typical deformation pattern for either the No. 8 or No. 11 bars, and while deformations were removed on the No. 5 bars to accommodate the grade stamp, the markings were staggered with such frequency that some portion of a grade marking would remain within the splice length on every specimen.

The cages were assembled using standard 8-in. and 10-in. wire ties. The reinforcement was cut with a band saw, and band saw cut ends of tension reinforcement were used within the splices to avoid inconsistencies in material properties and bar geometry common to the shear-cut ends of the as-delivered bars.

Prior to casting, dust was removed from reinforcing steel using compressed air. Rust was minor and not removed prior to casting.

Transverse anchor bars were welded within 2 in. of the end of the longitudinal reinforcement on all specimens, except those in two of the earlier test specimens, 8-5-OC0-1.5 and 8-5-XC0-1.5. An early specimen, not included in this report, exhibited bond failure near the loading apparatus at one end of the beam. The bond failure precipitated a shear failure in that specimen. The anchor bars used in subsequent specimens provided additional bearing area to ensure proper bar development at the termination of longitudinal steel. Additionally, the welded anchor bars kept the cage square and rigid during transport and concrete placement. The anchor bars were fillet welded to the longitudinal reinforcement with a high chromium E125 electrode.

Cover tolerances were achieved using standard steel reinforcement chairs attached directly to the longitudinal bars, a stirrup, or to a short piece of reinforcing bar of the size needed to maintain the appropriate cover of the supported longitudinal bar.

2.3.2 Formwork

Specimens were cast in individual forms constructed of ¾-in. plywood and 2x4s. The forms were protected using a multiple-layer polyurethane coating, and mineral oil was used as a release agent for all surfaces exposed to concrete. ⅜-in. all-thread low carbon steel rods were used in all specimens, with the exception of the two slab-beams in Series 2, to maintain correct width and transfer force to the form stringers. The rods passed through the specimen approximately 6 in. from the compression face of the beam at a spacing of 2 ft center-to-center throughout the entire length of the beam and remained in the concrete during the splice tests.

Because the test apparatus required the load rods be spaced at 36 in. transversely at the ends of the span, both specimens in Series 2 and specimen 11-8-XC2-2, a T-beam, required blockouts to reduce the section width at the loading points to accommodate the load rods. Descriptions of the reduced section are found in the specimen details located in Appendix B. No longitudinal bars were terminated due to these changes, and adequate cover was maintained for all longitudinal steel.

2.3.3 Casting and Curing Procedure

The beams were cast using readymix concrete. In most cases, they were cast in pairs. Workability was adjusted, as needed, by adding water that had been withheld during batching or by adding a HRWRA. Due to variability between concrete loads, all specimens using a specific mix design were not cast with identical batch quantities, although all 5 ksi and 8 ksi beams were each cast using the same two nominal mix designs. The nominal mix designs are reported in Table A.1 in Appendix A.

The beams were cast in two layers, beginning and ending at the ends of the beams, while placing the bottom and top layers of concrete in the splice regions of both beams from the middle portion of the batch to help ensure placement of the best quality concrete in the splice region. Concrete samples for strength specimens and standard concrete tests were taken in accordance with ASTM C 172, immediately before and after placing the first lift in both of the splice regions, and combined prior to testing the plastic concrete and casting the strength specimens. The concrete in the beams was consolidated using internal vibration after a complete layer had been placed.

After casting, beams were typically cured in the forms and covered with wet burlap and plastic sheeting on the exposed face until approximately three-quarters of the desired compressive strength had been reached, at which point the forms were stripped and the beams set on blocks to air-dry on all faces. Some specimens were stripped prior to attaining this strength and were instead completely covered in wet burlap and wrapped in plastic sheeting. During moist curing, beams were rewet a minimum of once per day.

2.3.4 Strength Specimens

Standard 6x12 in. concrete cylinders were cast in accordance with ASTM C 192 along with the splice specimens. The cylinders were stored next to the beams as they cured, and were stripped simultaneously with the beams.

Cylinders cast in disposable plastic molds were used to track the strength of the concrete as the beams cured. Three cylinders per beam were cast in steel molds; these cylinders were used to establish the concrete compressive strength when the beams were tested. The cylinders were capped in accordance with ASTM C 617 before testing. The cylinders were tested immediately after the completion of the splice test,

and strengths recorded to the nearest 10 psi, in accordance with ASTM C 39. Generally, if multiple beams were tested within a 24-hour period, the compressive strength of two beams cast simultaneously was treated as the same, and all cylinder strengths were averaged.

2.4 Specimen Measurements

2.4.1 Gross Section Properties

The beams were marked to indicate the locations of the load apparatus, pin and roller supports, ends of the splice region, and the beam centerline. All longitudinal measurements were taken from the centerline of the beam to eliminate any inconsistencies for beams slightly longer or shorter than the nominal length. The markings were 'PS' for the pedestal support, 'SR' to indicate the end of the splice region, and 'CL' for the centerline of the beam. The beams were also marked with cardinal directions for reference in photographs.

The width, height, and length were measured along the external faces of each specimen before testing. Height and width measurements were taken at 11 locations along all sides of each beam, including the pin and roller support locations, both ends of the splice region, and the centerline of the beam. Total beam length was typically measured on each side of the beam on both the compression and tension faces. To ensure accurate measurements, any excess concrete or surface variations were removed from corners of the beams with an abrasive block or angle grinder. Measurements were taken to $^{1}/_{32}$-in. accuracy.

2.4.2 Cover

Because of the inaccuracies inherent to measuring cover prior to casting, clear cover values are based on post-break measurements obtained from concrete debris broken at splice failure or with an air chisel after the completion of testing. Measurements were taken at each end of the splice because the moment is assumed to be highest there due to the self-weight of the beam. Concrete was also removed to expose the compression reinforcement in these locations.

Clear cover measurements taken at each splice end (based on original orientation at casting) include bottom cover to the tension reinforcement, external side cover, and top cover to the compression reinforcement. Additionally, the internal clear

spacing between splices was measured. Measurements to the tension reinforcement were made to the bar deformations, whereas the top cover was measured to the solid bar stock. All concrete cover measurements were made with calipers accurate to 0.001 in.

2.4.3 Bar Deformation Properties

The bar deformation characteristics were measured and the relative rib areas calculated for the Grade 100 ASTM A 1035 bars used in this study. The results are presented in Table A.4 in Appendix A. Relative rib area is a measure of the bearing area of deformations on a reinforcing bar normalized to the surface area of that bar between deformations. Relative rib area was measured in accordance with ACI 408.3-01 / 408.3R-01.

Six-inch digital calipers were used to determine the average width and spacing of the deformations. A knife-edge dial gage spanning two deformations was used to determine the deformation height in five places between the ribs. All measurements were taken on a minimum of five deformations per bar to ensure consistency. Measurements were accurate to 0.001 in. The relative rib areas were determined to be 0.0767 for No. 5 bars, 0.0838 for No. 8 bars, and 0.0797 for No. 11 bars. The three bars are shown in Figure 2.4.

Figure 2.4 – Photograph of No. 5, 8, and 11 MMFX Grade 100 reinforcement

2.5 Test Setup

2.5.1 General

All specimens were designed to be tested in four-point bending. Prior to testing, each beam was inverted from its casting position. This was done by rotating the beams while they were supported on longitudinal No. 8 bars cast into and projecting out of the end of the beams. The beams were initially cast tension-face down to avoid any top-bar effect on the primary reinforcement, which is known to reduce bond strength of reinforcing bars. They were tested in an inverted position for safety and ease of marking cracks.

As shown in Figure 2.5, the two central reactions were provided by pin and roller supports made of cold-worked, solid round-stock steel bars in contact with the compression face through 1-in. thick cold-rolled bearing plates. The pin and roller were mounted on concrete pedestals that were, in turn, supported by a 2-ft thick reinforced concrete structural floor. All surfaces involved in load transfer were covered with a layer of Hydrostone, a 10,000 psi high strength gypsum plaster, which is used to prevent movement between the surfaces and ensure even load distribution.

Beams in Series 3 and 4 were supported by a 6-in. diameter roller and pin, both 12 in. long, with appropriately sized bearing plates above and below, with the exception of specimen 8-5-XC2-1.5, a T-beam. All other beams, including both T-beams, were supported on 30-in. long, 2⅝-in. diameter round-stock, on 30 x 6-in. bearing plates. Pin supports were fabricated by welding the round-stock to the lower bearing plate, allowing no translation between the two.

At each end of the beam, loads were applied through a W8x48 steel spreader beam spanning the tension face. Each spreader beam was connected to two 1½-in. diameter high-yield threaded rods which were passed through stiffened openings in the wide flange section. These rods were pulled downward through the structural concrete floor by load-equalized hydraulic jacks connected to a central pump. Load cells on each of the four load rods were independently calibrated from 0 to 100 kips, approximately twice the highest load on a single rod required for any test.

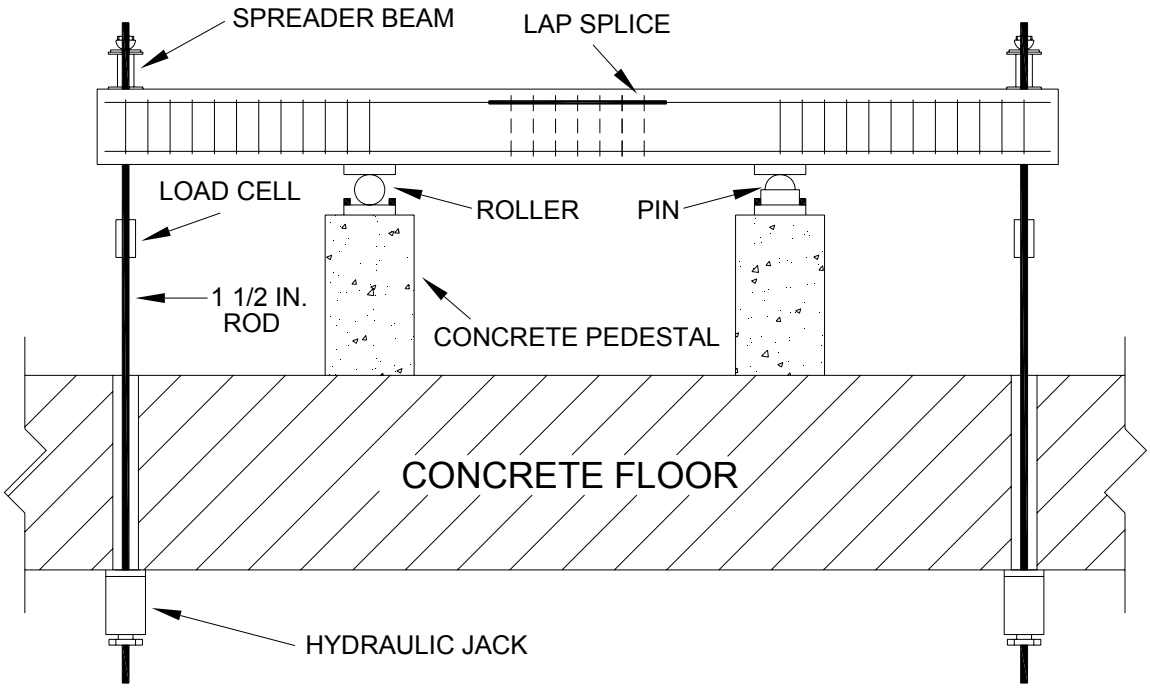

Figure 2.5 – Schematic of testing setup and loading method

2.5.2 Instrumentation

Three linear variable differential transformers (LVDTs) were used to record the vertical beam deflections; one at midspan and one at each load application point at the end of the span. A dial gage was attached to each LVDT stand so that beam deflections could also be recorded by hand.

The applied load was measured using load cells located on each rod consisting of a group of four strain gages arranged in a full Wheatstone bridge. Readings from the LVDTs and load cells were monitored and recorded using a data acquisition (DA) system. The DA system recorded readings from the LVDTs and the load cells at a rate of 4 Hz. Figure 2.6 shows a photograph of a beam specimen in the testing setup.

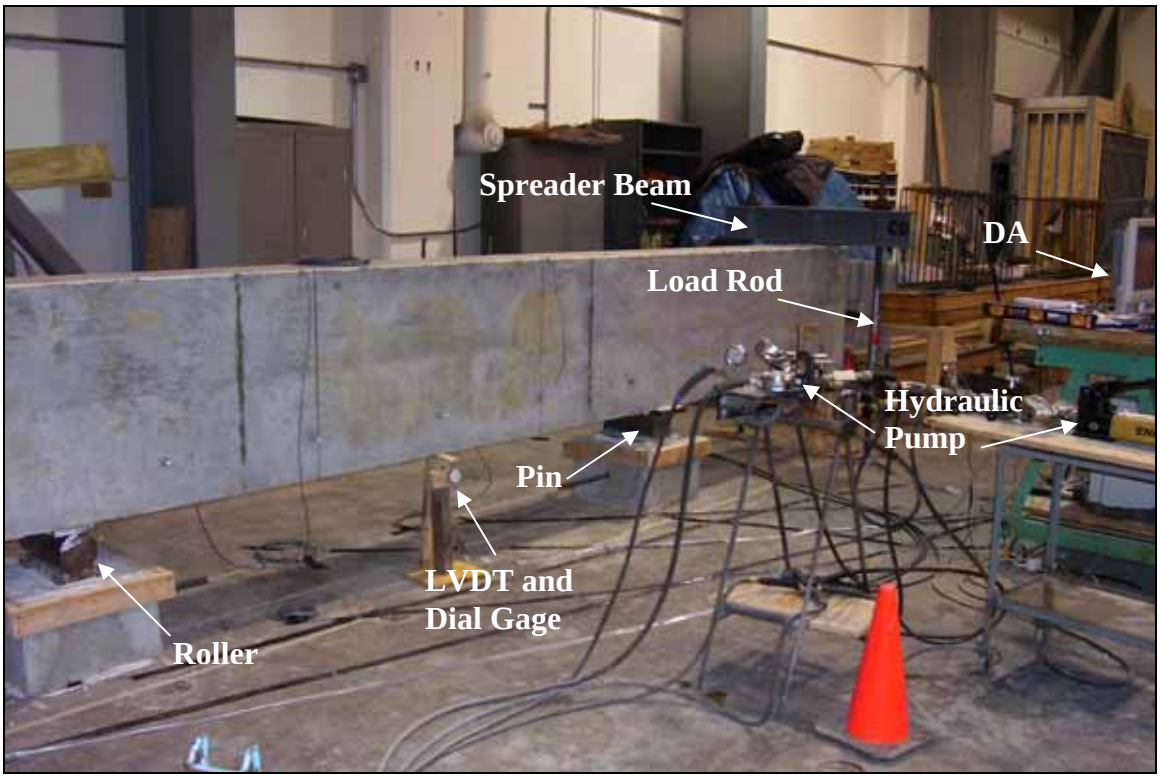

Figure 2.6 – Photograph of testing setup

Within each specimen, four 120Ω ¼-in. strain gages with attached leads were bonded to the primary tension reinforcement. One strain gage was placed on each spliced bar approximately two inches outside the end of the splice. One deformation on each No. 8 and 11 bar was removed using low-heat grinding and polishing to provide a level surface for attaching the strain gage. No. 5 bars typically required the removal of two deformations. Strain gages were applied and sealed following the manufacturer's recommended procedures for submersion in concrete. The coating used to seal the strain gages typically covered a number of deformations, all outside of the splice region. Strain gages were read using strain indicator boxes.

2.6 Test Procedure

Prior to each test, the double acting jack system was pumped fully in reverse, after which all slack was taken out of the load rods by tightening the nuts until each load rod was almost engaged with the fully retracted hydraulic jacks. This was done to ensure even loading across all four rods.

After zeroing all LVDT, load cell, and strain gage readings on the DA system and strain indicator boxes, zero readings were recorded for each of the three dial gages. Load was applied using a manually-controlled hydraulic pump. Pauses were incorporated in the loading sequence at predetermined load levels to visually inspect the beam, mark visible cracks, measure crack widths using crack comparators, and to record strain and dial gage readings.

The initial load increment was always half of the estimated cracking load to ensure that all instruments and the hydraulic system were operating properly, while the second load step reached the estimated cracking load. The total number and size of load increments varied depending on the estimated capacity of the specimen being tested. Pauses typically were limited to 4 minutes or less. Following specimen failure, the jacks were pumped in reverse until all load was removed from the rods and the jacks were fully retracted.

Due to the brittle nature and large amount of stored energy released in splice failures, the final load step at which cracks were marked and measured was typically set as ⅔ of the estimated failure load. After this point, the load was increased steadily until failure. The total test duration varied from 18 to 64 minutes for beams 5-5-OC0-2d_b and 11-8-OC0-2, respectively, and averaged 37 minutes.

2.7 Section Analysis

2.7.1 General

Loads, moments, and stresses for the beams were calculated using a two-dimensional analysis in which loads and reactions were assumed to act along the longitudinal centerline of the beam. Reactions and moments were based on load cell readings and the weight of the loading assemblies. The self-weight of the beam was included in the calculations based on average beam dimensions and an assumed density of 150 pcf. Given that specimens generally experienced nearly identical moments at both ends of the splices, splitting failures were assumed to initiate from the splice end with the smallest measured cover dimension.

The test specimens were evaluated using a cracked section analysis with a linear strain distribution throughout the cross-section. The beams were analyzed by both strength and moment-curvature methods for comparison. The moment-curvature

method uses a nonlinear stress-strain curve for the concrete, while the strength method uses an equivalent stress block. Good agreement in calculated values was noted between the two methods; unless stated otherwise, all bar stress values reported are based on the moment-curvature method. It should be noted that bar stresses based on the moment-curvature method exceeded those obtained using the strength method by 1.2 to 3.8 ksi, with an average of 2.9 ksi. Figure 2.7, modified from Nawy (2003), is a representation of the moment-curvature and strength methods of section analysis.

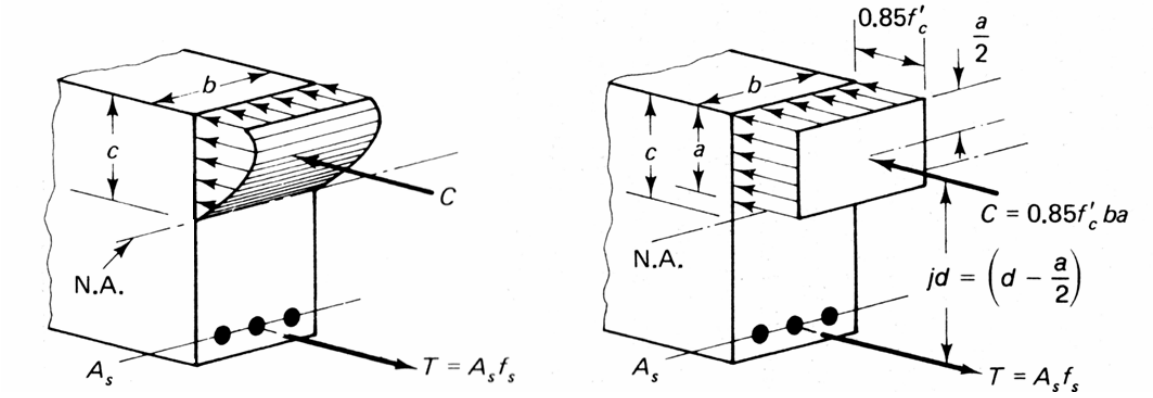

Figure 2.7 – Moment-curvature and strength analysis [after Nawy (2003)]

2.7.2 Reinforcing Steel

The steel tensile stress f_s (ksi) of MMFX Grade 100 reinforcing steel was estimated using the stress-strain curves given in Eq. (2.3) and (2.4) provided by UT (Glass 2007). Equation (2.3) was used for both No. 5 and 8 bars, while Eq. (2.4) was used for No. 11 bars. The compression steel is standard Grade 60 steel and is assumed to follow the bi-linear stress-strain curve given in Eq. (2.2). Figure 2.8 shows the steel stress-strain curves.

$$f_s = 29000 \times \varepsilon_s \leq 60 \text{ ksi} \tag{2.2}$$

$$f_s = 156 \times \left(1 - e^{-220\varepsilon_s}\right) \tag{2.3}$$

$$f_s = 162 \times \left(1 - e^{-235\varepsilon_s}\right) \tag{2.4}$$

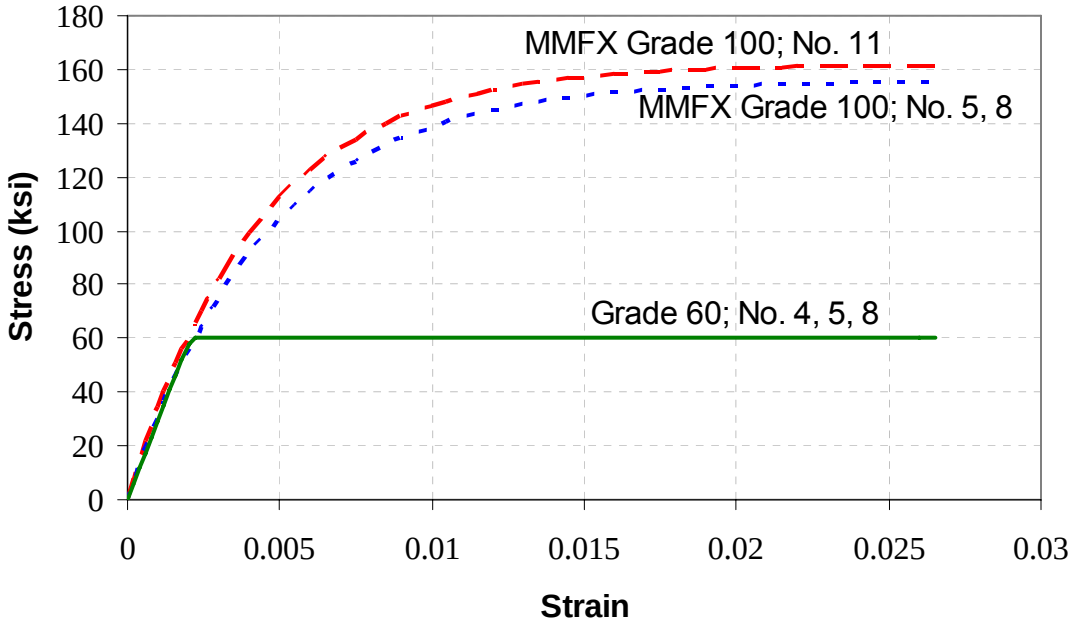

Figure 2.8 – Stress-strain curves for Grade 60 and MMFX Grade 100 steels

2.7.3 Concrete

Evaluations made with the strength method used the Whitney stress block and the values of β_1 provided in ACI 318-05. Concrete stress f_c and strain ε_c in the moment-curvature calculations were estimated using the modified concrete stress-strain relationship developed by Hognestad (1951). Both analyses neglect the tensile strength of the concrete. The modified Hognestad relationship is listed as Eq. (2.5). Figure 2.9 shows example stress-strain curves for 5 and 8 ksi concrete.

$$f_c = \begin{cases} f_c'' \left[2\left(\frac{\varepsilon_c}{\varepsilon_0}\right) - \left(\frac{\varepsilon_c}{\varepsilon_0}\right)^2 \right] & \text{for} \quad \varepsilon_c \le \varepsilon_0 \\ f_c'' \left[0.15\left(\frac{\varepsilon_0 - \varepsilon_c}{\varepsilon_{cu} - \varepsilon_0}\right) - 1 \right] & \text{for} \quad \varepsilon_c \ge \varepsilon_0 \end{cases} \tag{2.5}$$

$$f_c'' = 0.85 f_c' \tag{2.5a}$$

$$\varepsilon_0 = \frac{1.7 f_c'}{E_c} \tag{2.5b}$$

$$\varepsilon_{cu} = 0.0038 \tag{2.5c}$$

$$E_c = 1.8 \times 10^6 + 460 f_c' \tag{2.5d}$$

where:

f_c = concrete stress, psi

f_c' = concrete compressive strength, psi

f_c'' = peak concrete stress, psi

ε_c = concrete strain

ε_0 = concrete strain at peak stress

ε_{cu} = ultimate concrete strain at crushing

E_c = approximate concrete modulus of elasticity, psi

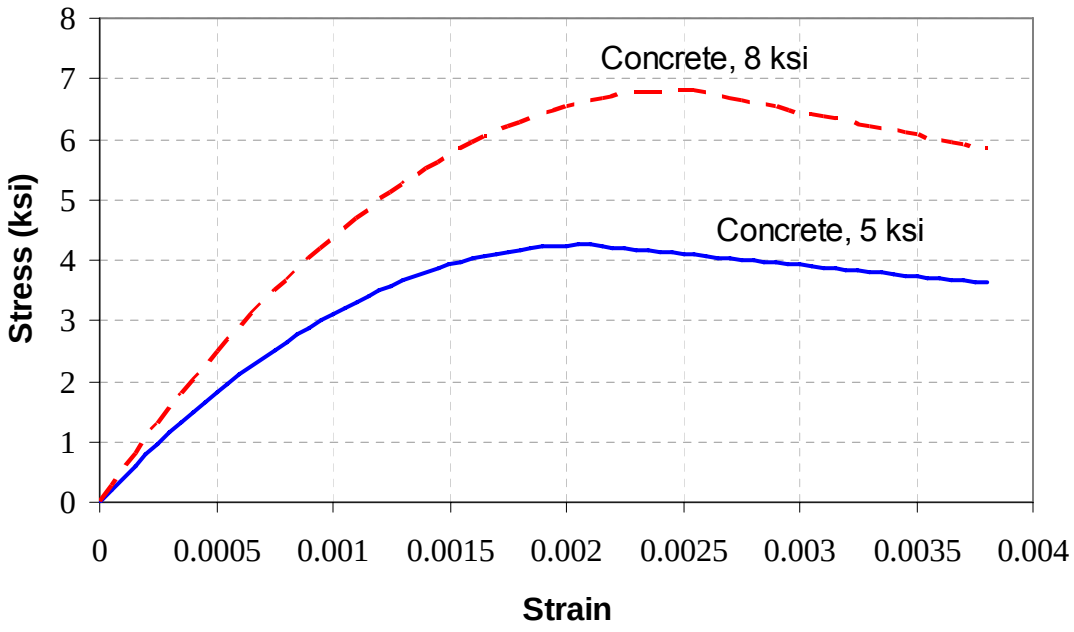

Figure 2.9 – Hognestad stress-strain curves for f_c' = 5 and 8 ksi

3.0 Test Results for KU Specimens

3.1 General

The twenty-two beam splice specimens tested at KU were evaluated with respect to the observed failure mode, load-deflection behavior, comparison of the test and predicted bar stresses, and crack patterns. The results reported here are those typical for the majority of the tests. Detailed test results are presented in Appendix B. Table 3.1 summarizes the concrete strength, cover and spacing measurements, splice lengths, quantity of confining transverse reinforcement, and the bar stresses at failure, as predicted by ACI 408R-03 and calculated based on the strength or moment-curvature method for the test specimens.

Table 3.1 –Summary of KU beam-splice specimen test results

Group	Specimen	Bar Size	f'_c	c_b	c_{so}	c_{si}	Splice Length, ℓ_s	Stirrups Confining Splice	Predicted Failure Stress (ACI 408R)	Actual Failure Stress	
										Strength	Moment Curvature
		(No.)	(psi)	(in.)	(in.)	(in.)	(in.)	(ea.)	(ksi)	(ksi)	(ksi)
1A	**5-5-OC0-3/4**	5	5,490	0.73	1.08	1.02	32	0	80.3	73.9	77.0
1B	**5-5-XC0-3/4**		4,670	0.66	0.92	1.09	43	0	90.7	79.5	82.2
2A	**5-5-OC0-2db**		5,490	1.05	3.72	3.67	18	0	77.4	83.1	86.9
2B	**5-5-XC0-2db**		4,670	0.98	3.80	3.64	25	0	89.8	87.8	91.2
3A	**8-5-OC0-1.5**	8	5,260	1.34	1.41	3.63	47	0	77.0	75.1	78.1
	8-5-OC1-1.5		4,720	1.54	1.51	3.32		4	99.5	122.1	123.5
	8-5-OC2-1.5		6,050	1.34	1.44	3.37		8	127.3	125.4	127.3
3B	**8-5-XC0-1.5**		5,940	1.35	1.41	3.62	63	0	99.5	87.0	90.0
	8-5-XC1-1.5		4,720	1.46	1.52	3.36		4	117.9	127.5	128.7
	8-5-XC2-1.5		5,010	1.30	1.53	3.23		8	135.5	141.4	143.0
4A	**8-8-OC0-2.5**		8,660	2.25	2.25	2.64	27	0	77.7	75.9	79.5
	8-8-OC1-2.5		7,790	2.37	2.19	2.54		2	89.5	85.3	88.7
	8-8-OC2-2.5		7,990	2.16	2.28	2.63		5	100.7	112.3	115.0
4B	**8-8-XC0-2.5**		7,990	2.32	2.38	2.61	36	0	96.1	87.7	91.1
	8-8-XC1-2.5		7,790	2.46	2.35	2.48		2	110.9	108.1	111.0
	8-8-XC2-2.5		8,660	2.25	2.44	2.57		5	129.3	114.5	117.4
5A	**11-8-OC0-2**	11	9,370	1.82	1.83	6.89	58	0	78.9	64.5	67.9
	11-8-OC1-2		9,370	1.55	1.68	7.25		4	94.6	91.7	95.5
	11-8-OC2-2		8,680	1.82	1.94	6.95		9	122.4	120.3	123.5
5B	**11-8-XC0-2**		9,910	1.76	1.87	7.30	79	0	99.1	75.2	78.9
	11-8-XC1-2		9,910	1.94	2.02	6.98		4	126.2	103.2	106.9
	11-8-XC2-2		8,680	1.71	2.12	6.88		9	140.6	134.4	137.3

3.2 Failure Mode

The 22 specimens tested at KU failed in bond due to splitting of the concrete cover surrounding the tension lap splices.

3.2.1 Unconfined Splice Specimens

Beams without confining transverse reinforcement typically exhibited characteristics of a brittle failure and abruptly lost all load-carrying capacity. During testing, it was observed that the greater the failure load and likewise the stored energy, the greater the likelihood that the splices would fail explosively. Specimens with low total loads and lower concrete strength also exhibited brittle splice failures, but were much less likely to fail in an explosive manner.

During testing, it was observed that the exterior two (of four) splices in beams 5-5-OC0-2d_b and 5-5-XC0-2d_b failed prior to the ultimate failure of the specimen. These two specimens were slab beams with four splices apiece and no confining transverse reinforcement. After initial failure, the load dropped slightly, but the beam again picked up load until the inner splices failed. The peak load is used for analysis.

3.2.2 Confined Splice Specimens

Beams with confining transverse reinforcement in the splice region typically failed more gradually and exhibited far greater ductility than beams without confining transverse reinforcement. Beams with confining transverse reinforcement consistently developed longer splitting cracks prior to failure and often could be heard cracking near the ultimate load. Although failure was still brittle for beams with confined splices, the large increase in ductility provided by the transverse reinforcement is desirable. Examples of the increases in ductility are outlined in the following section on Load-Deflection Behavior and also in the test details in Appendix B.

3.3 Load-Deflection Behavior

The load-deflection behavior for each group of specimens was examined to evaluate the effect of splice strength on the load carrying and deformation capacity of the specimens. For all load-deflection plots, the total deflection of the beam is plotted versus the total load. As can be observed in the load-deflection behavior of the specimens in Group 3B, displayed in Figure 3.1, adding confining transverse

reinforcement not only increases the splice strength but also deformation capacity. The additional load capacity and ductility are directly related to the quantity of confining transverse reinforcement. Specimens with unconfined splices (that is, without confining transverse reinforcement) failed in a brittle manner at significantly lower bar stresses and smaller overall beam deflections than those with confinement, while additional confinement further increased the bar stress and beam deflection before failure.

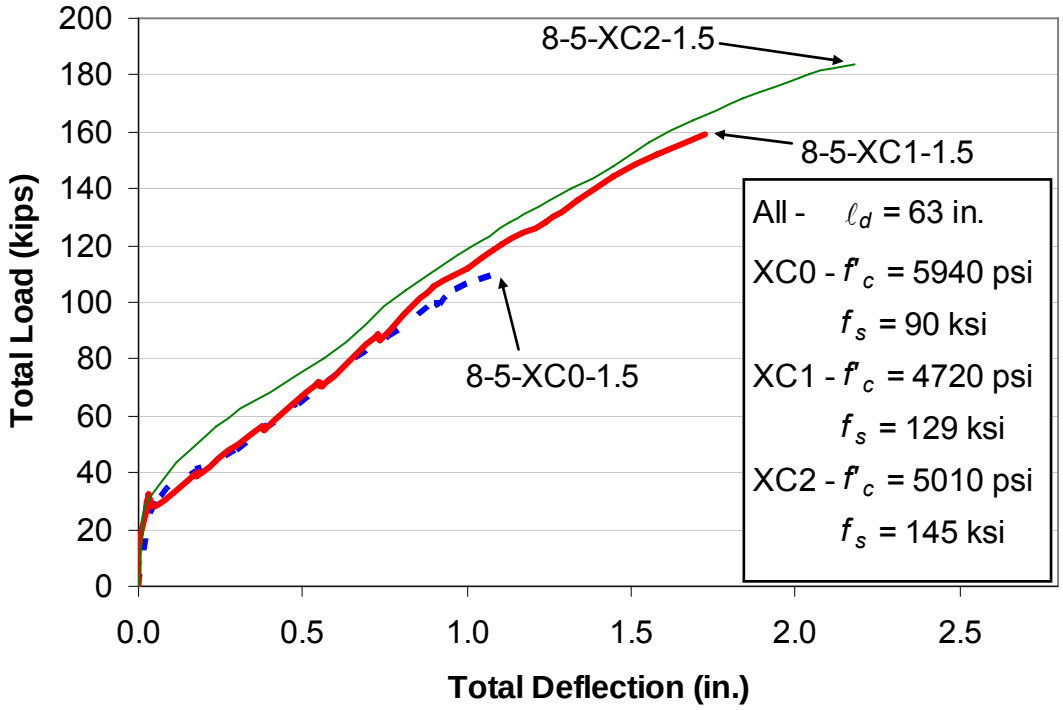

Figure 3.1 – Load-deflection behavior for specimens in Group 3B

Figure 3.1 shows the trend of an increasing rate of deflection with incremental increases in load capacity. This is attributed to a continuing loss of stiffness as flexural cracks extend deeper into the specimen, reducing the effective moment of inertia.

Load-deflection plots are shown for all specimens in Appendix B.

3.4 Calculated and Measured Bar Stresses

The calculations and comparisons made in this study are based on bar stresses calculated using the moment-curvature method. To determine the effects of reinforced

concrete behavior not included in the assumptions of the moment-curvature method, most notably bar slip, four strain gages were applied to the primary tension bars immediately outside of the splices in each specimen as a means to measure actual bar stress. The measured bar stress is compared to the calculated bar stress at or near failure for Series 5 in Table 3.2. The "measured bar stress" is calculated based upon the measured strain and the same stress-strain curve as used for the moment-curvature calculations. As can be seen, the measured stresses closely correlate to the calculated stresses. The measured stresses are, on average, 1.7% higher than the calculated stresses, and range from 2.8% lower to 5.6% higher.

Table 3.2 – Peak bar stress at mean failure load for Series 5 specimens

Beam ID	Load (kips)	Calculated Stress* (ksi)	Measured Stress (ksi)	Meas.-to-Calc. Difference (ksi)	Meas.-to-Calc. Difference (%)
11-8-OC0-2	117	68	71	2.7	4.0%
11-8-XC0-2	136	79	83	4.4	5.6%
11-8-OC1-2	168	95	99	3.4	3.5%
11-8-XC1-2	185	107	104	-3.0	-2.8%
11-8-OC2-2	212	124	123	-0.1	-0.1%
11-8-XC2-2	242	137	137	-0.3	-0.2%

* Based on moment-curvature method

The measured stresses based on the strain gage readings for Groups 5A and 5B are shown in Figures 3.2 and 3.3, respectively. The average strain gage reading from each test is shown in these graphs, omitting any gages that vary significantly from the others in the group. It should be noted that specimen 11-8-OC2-2 (Figure 3.2) was loaded to roughly 48 kips total load and subsequently unloaded and reloaded due to technical problems with the hydraulic system. The graph shows only the reloading, and thus does not display the low stress prior to cracking, indicated in all other records by the much shallower slope at low load levels. The final failure data points, indicated by asterisks, are calculated based on moment curvature and included for comparative purposes.

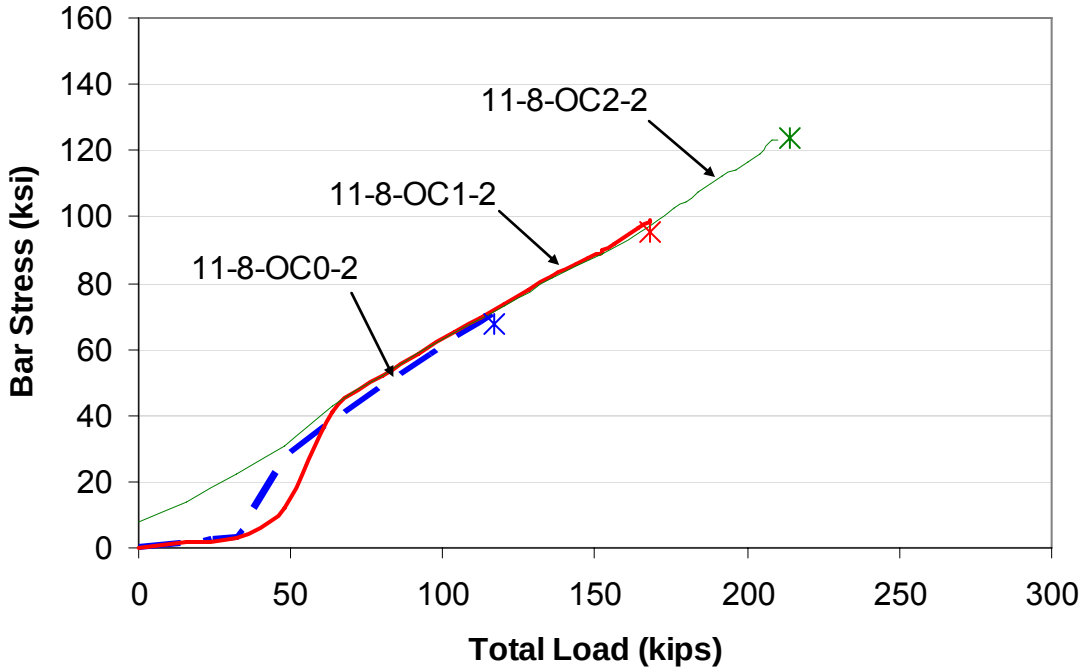

Figure 3.2 – Measured bar stress vs. total beam load for Group 5A specimens

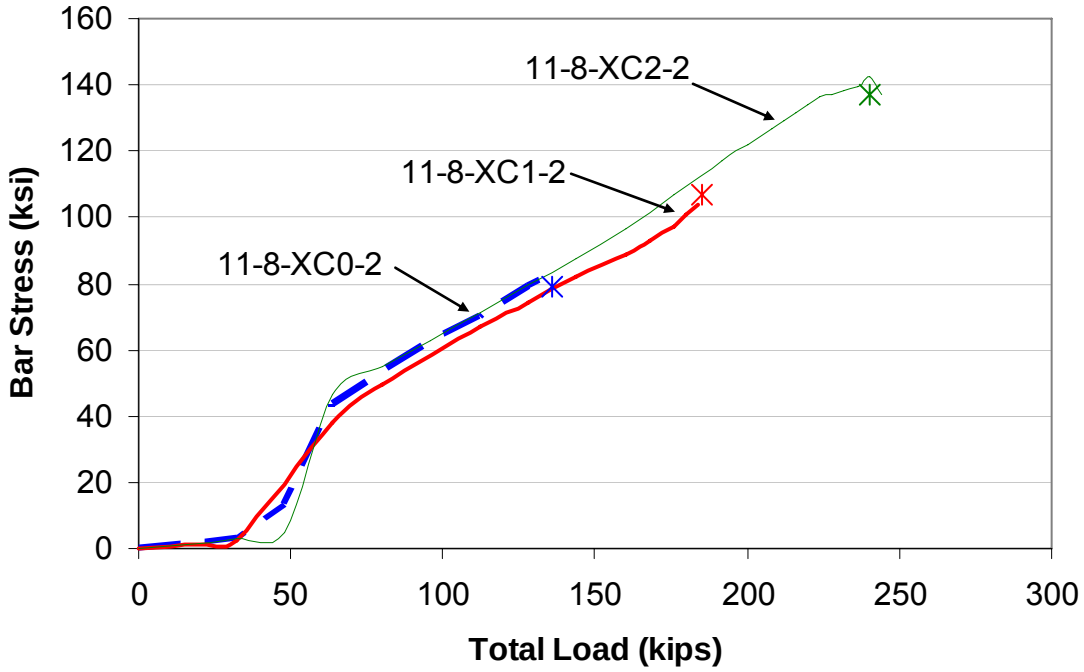

Figure 3.3 – Measured bar stress vs. total beam load for Group 5B specimens

3.5 Cracking

During testing, flexural, splitting, and shear cracks formed. Flexural cracks were observed first, while shear cracks and bond splitting cracks developed as loading continued. Crack patterns typically grew complicated at high load levels around sites of internal discontinuity, such as the location of reinforcing bar chairs and strain gages. A card-type clear plastic crack comparator was used to measure crack width.

3.5.1 Flexural Cracks

Flexural cracks were first observed over the supports or at one or both ends of the splice region. Most cracks formed in the early stages of loading. In the later stages of loading, fewer new cracks formed as the initial cracks grew. Flexural cracks often formed at the locations of the stirrups used as confining transverse reinforcement in the splice region, and the widest cracks formed at the ends of the splices.

Figure 3.4 shows the maximum flexural crack widths as a function of bar stress at the ends of the splice for the loads that produced stresses bounding values of both 40 and 67 ksi. The data are presented in Table B.2 in Appendix B. The values 40 and 67 ksi are equal to $\frac{2}{3}f_y$ for f_y = 60 and 100 ksi, respectively, the service stress upon which the crack control provisions (expressed as reinforcement spacing criteria) in Section 10.6.4 of ACI 318-05 are based. Figure 3.4 also shows the best-fit lines based on the two data points from each test adjacent to 40 and 67 ksi, along with lines representing the 90% upper bound on crack width, established using a student t-distribution-based prediction interval with n-2 degrees of freedom (10%, n = 41 at 40 ksi) (10%, n = 30 at 67 ksi). Three visually identified outliers were removed from the 40 ksi dataset. At 40 and 67 ksi, these upper-bound lines give the crack widths corresponding to a 10% probability of exceedance. The slope, intercept, and interpolated crack widths for the best-fit lines are shown in Table 3.3. The mean and upper-bound crack widths are 0.0014 in. and 0.017 in., respectively, for a bar stress of 40 ksi, and 0.028 and 0.044 in. for a bar stress of 67 ksi. The crack widths are reasonable and approximately match expectations for a service load stress of 40 ksi, representing, respectively, the maximum crack widths for interior and exterior exposure in ACI 318-99 and earlier. The crack widths at 67 ksi, however, are significantly above

these values and greater than would be expected based on a linear relationship between bar stress and crack width.

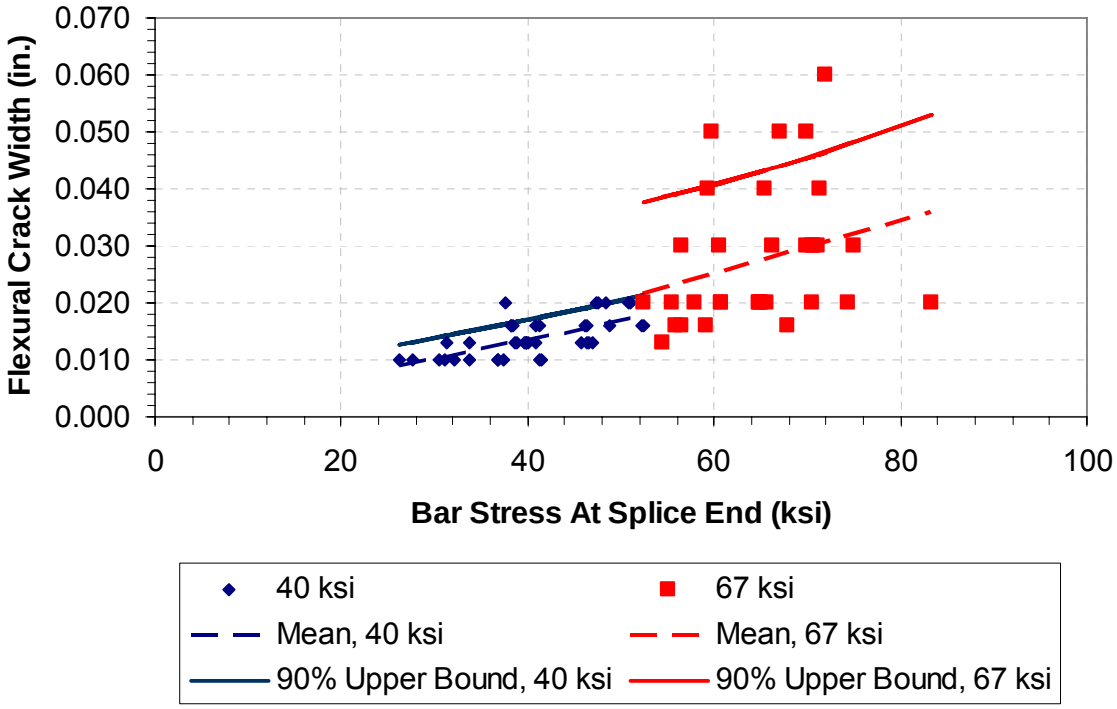

Figure 3.4 – Maximum flexural crack widths at bar stresses bounding 40 and 67 ksi in KU beam-splice tests shown with median and 90% upper-bound regression lines

Table 3.3 – Summary of crack widths at 40 and 67 ksi for KU specimens

Bar Stress At Crack	Best-fit Linear Regression Prediction		Flexural Crack Width	
	Slope	Intercept	Average, $w_{cr\text{-}avg}$	90% Upper Bound, $w_{cr\text{-}90\%}$
	(in./ksi)	(in.)	(in.)	(in.)
40 ksi	0.0003	0.0005	0.014	0.017
67 ksi	0.0005	-0.0030	0.028	0.044

3.5.2 Splitting Cracks

Splitting cracks generally propagated from flexural cracks and first appeared at the splice ends, continuing toward the centerline of the beam. Splitting cracks were most commonly found on the tension face of the beam, although side splitting cracks often formed at higher load levels. Figure 3.5 shows bottom (as cast) and side splitting cracks that formed on specimen 8-8-XC1-2.5. Table 3.4 summarizes the loads, bar stresses, and flexural crack widths at the initiation of splitting cracks, excluding

specimens in which no splitting cracks were observed before the final load step. Splitting cracks were initially observed at tensile bar stresses of about 40 ksi in most specimens, but began appearing at bar stresses as high as 85 and 55 ksi in a test specimen with No. 8 and No. 11 bars, respectively.

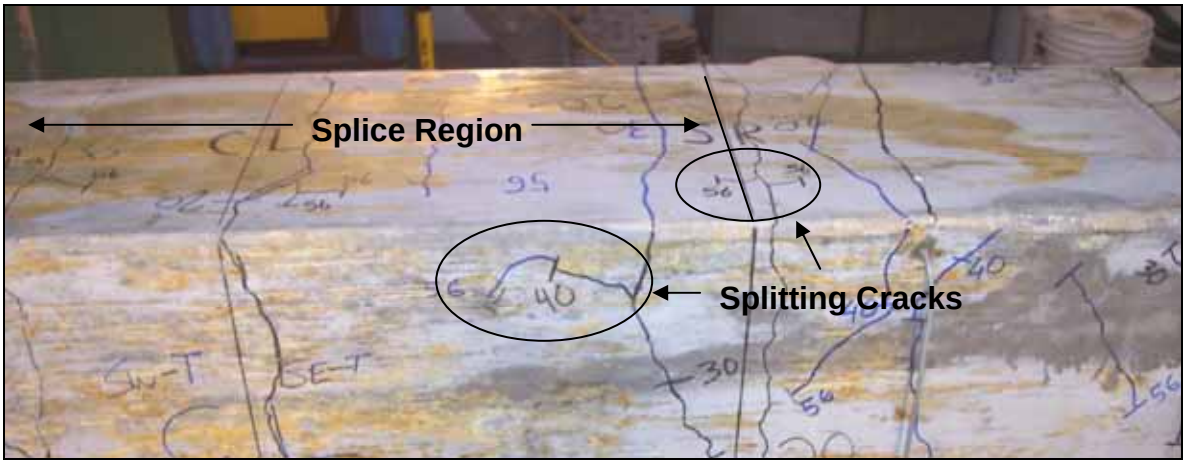

Figure 3.5 – Splitting cracks in specimen 8-8-XC1-2.5 at 56 kips total load

Table 3.4 – Load and stresses in the spliced bars at initiation of splitting cracks

Beam ID	f'_c	Nominal Section, b x h	Minimum Design Cover	Splice Length	Stirrups Confining Splice	At Splitting Crack Initiation		
						Total Load	Splice Stress	Flexural Crack Width
	(psi)	(in. x in.)	(in.)	(in.)	(ea.)	(kips)	(ksi)	(in.)
5-5-OC0-3/4	5,490	14 x 20	0.75	32	0	---	---	---
5-5-XC0-3/4	4,670			43	0	52	59	0.016
5-5-OC0-2d_b	5,490	35 x 10	1.25	18	0	---	---	---
5-5-XC0-2d_b	4,670			25	0	---	---	---
8-5-OC0-1.5	5,260	14 x 30	1.5	47	0	48	40	0.013
8-5-0C1-1.5	4,720				4	48	40	0.010
8-5-OC2-1.5	6,050				8	80	65	0.020
8-5-XC0-1.5	5,940			63	0	48	40	0.013
8-5-XC1-1.5	4,720				4	72	59	0.030
8-5-XC2-1.5	5,010				8	80	65	0.020
8-8-OC0-2.5	8,660	14 x 21	2.5	27	0	---	---	---
8-8-OC1-2.5	7,790				2	30	39	0.013
8-8-OC2-2.5	7,990				5	44	55	0.020
8-8-XC0-2.5	7,990			36	0	32	41	0.016
8-8-XC1-2.5	7,790				2	40	51	0.020
8-8-XC2-2.5	8,660				5	68	85	0.030
11-8-OC0-2	9,370	24 x 26	2	58	0	64	38	0.016
11-8-OC1-2	9,370				4	64	38	0.020
11-8-OC2-2	8,680				8	64	38	0.016
11-8-XC0-2	9,910			79	0	64	38	0.016
11-8-XC1-2	9,910				4	64	40	0.013
11-8-XC2-2	8,680				8	80	48	0.020

In beams with confining transverse reinforcement, splitting cracks typically initiated at higher loads than for beams without confinement. Generally, splitting cracks initiated in unconfined beams at a bar stress of about 40 ksi, while splitting crack initiation in confined beams occurred at bar stresses between 40 and 85 ksi. In four beams with unconfined splices, splitting cracks were not observed before the last load step at which it was safe to approach the beam. Three of these four were the slab specimens with No. 5 tension reinforcement.

During tests on Series 5 specimens (beams with No. 11 bars), splitting cracks were also noted near the supports at higher bar stresses. After testing of Series 5 specimens with high confinement, splitting cracks were observed along the majority of the beams, even away from the regions of highest moment. Splitting cracks were noted within one foot of the loading apparatus at endspan on specimen 11-8-XC2-2.

3.6 Comparisons with Development Length Equations

In this section, the test results are compared to the equations that relate bar stress with development length in ACI 318-05 and ACI 408R-03 for bottom-cast bars in normalweight concrete. These equations, expressed in terms of bar stress, are, respectively:

$$f_s = \frac{40}{3} \times \frac{\ell_d}{d_b} \times \frac{\sqrt{f'_c}}{\psi_s} \times \left(\frac{c + K_{tr}}{d_b} \right) \tag{3.1}$$

$$K_{tr} = \frac{A_{tr} f_{yt}}{1500sn} \tag{3.1a}$$

$$f_s = \left(76.3 \frac{\ell_d}{d_b} \left(\frac{c\omega + K_{tr}}{d_b} \right) + 2400\omega \right) f_c'^{1/4} \tag{3.2}$$

$$K_{tr} = \left(\frac{0.52 t_r t_d A_{tr}}{sn} \right) f_c'^{1/2} \tag{3.2a}$$

$$\omega = 0.1\frac{c_{max}}{c_{min}} + 0.9 \leq 1.25 \quad (3.2b)$$

$$t_r = 9.6R_r + 0.28 \quad (3.2c)$$

$$t_d = 0.72d_b + 0.28 \quad (3.2d)$$

where:

A_b = nominal cross-sectional area of the reinforcement being developed, in.^{2}

A_{tr} = total cross-sectional area of all transverse reinforcement, in.^{2}

c_b = cover of reinforcement being developed, measured to tension face of member, in.

c_{max} = maximum value of c_s or c_b, in.

c_{min} = minimum value of c_s or c_b, in.

c_s = minimum value of c_{si} + 0.25 in. or c_{so}, in.

c_{so} = side cover of reinforcing bars, in.

c_{si} = half the clear spacing between reinforcing bars, in.

d_b = nominal bar diameter, in.

f'_c = specified compressive strength of concrete, psi

f_s = bar stress, psi

f_{yt} = yield strength of the tensile reinforcement (taken as 60,000 psi in this study)

ℓ_d = development length, in.; taken as equal to splice length ℓ_s

N = number of transverse stirrups within the splice length

n = number of bars being developed or spliced along plane of splitting

R_r = relative rib area, ratio of projected rib area normal to bar axis to product of nominal bar perimeter and average center-to-center rib spacing

s = average center-to-center spacing of transverse reinforcement within ℓ_d or ℓ_s, taken as ℓ_s/N for comparison with test results

ψ_s = reinforcement size factor = 1.0 for bar sizes greater than No. 7 and 0.8 for No. 6 and smaller

Equations (3.1) and (3.2) are used as to predict bar stress at splice failure. Both equations were developed based on test results in which splitting failure, rather than pullout, governs. Accordingly, the confinement terms $\left(\frac{c + K_{tr}}{d_b}\right)$ and $\left(\frac{c\omega + K_{tr}}{d_b}\right)$ are limited, respectively, to values of 2.5 for Eq. (3.1) and 4.0 for Eq. (3.2). In this study, the splice strengths of specimens with confinement terms greater than the respective limits of 2.5 and 4.0 were calculated using the limits.

Comparisons between the test results and the corresponding predictions are presented separately for unconfined and confined splices in Tables 3.5 and 3.6, respectively. Also reported are the average, standard deviation, range, and coefficient of variation of the test/prediction ratios for both Eq. (3.1) and (3.2).

Table 3.5 – Comparisons of test and predicted (ACI 318 and 408R) bar stresses at failure for unconfined KU beam-splice specimens

Specimen	Test	ACI 318-05		ACI 408R-03	
	Stress (ksi)	Stress (ksi)	Test/ Prediction	Stress (ksi)	Test/ Prediction
5-5-OC0-3/4	77.0	105.3	0.73	80.3	0.96
5-5-XC0-3/4	82.2	121.6	0.68	90.7	0.91
5-5-OC0-2d_b	86.9	77.6	1.12	77.4	1.12
5-5-XC0-2d_b	91.2	93.9	0.97	89.8	1.01
8-5-OC0-1.5	78.1	83.5	0.93	77.0	1.01
8-5-XC0-1.5	90.0	119.6	0.75	99.5	0.90
8-8-OC0-2.5	79.5	83.8	0.95	77.7	1.02
8-8-XC0-2.5	91.1	107.3	0.85	96.1	0.95
11-8-OC0-2	67.9	94.9	0.72	78.9	0.86
11-8-XC0-2	78.9	129.9	0.61	99.1	0.80
			0.83	Average	0.95
			0.16	Std. Dev.	0.09
			0.19	Coef. Var.	0.10
			1.12	Maximum	1.12
			0.61	Minimum	0.80

Table 3.6 – Comparisons of test and predicted (ACI 318 and 408R) bar stresses at failure for confined KU beam-splice specimens

Specimen	Test	ACI 318-05		ACI 408R-03	
	Stress (ksi)	Stress (ksi)	Test/ Prediction	Stress (ksi)	Test/ Prediction
8-5-OC1-1.5	123.5	107.6	1.15	99.5	1.24
8-5-XC1-1.5	128.7	142.2	0.90	117.9	1.09
8-5-OC2-1.5	127.3	122.2	1.04	127.3	1.00
8-5-XC2-1.5	143.0	148.6	0.96	135.5	1.06
8-8-OC1-2.5	88.7	79.4	1.12	89.5	0.99
8-8-XC1-2.5	111.0	105.9	1.05	110.9	1.00
8-8-OC2-2.5	115.0	80.4	1.43	100.7	1.14
8-8-XC2-2.5	117.4	111.7	1.05	129.3	0.91
11-8-OC1-2	95.5	105.8	0.90	94.6	1.01
11-8-XC1-2	106.9	160.8	0.66	126.2	0.85
11-8-OC2-2	123.5	127.7	0.97	122.4	1.01
11-8-XC2-2	137.3	164.1	0.84	140.6	0.98
			1.00	Average	0.99
			0.20	Std. Dev.	0.08
			0.20	Coef. Var.	0.08
			1.43	Maximum	1.14
			0.66	Minimum	0.85

The comparisons show that the ACI 408R-03 equation [Eq. (3.2)] provides a better match with the KU data, with less scatter, than the ACI 318-05 equation [Eq. (3.1)] for unconfined splices and a similar average value with significantly less scatter for confined splices. The mean test/prediction ratios are lower for ACI 318-05 for unconfined splices, 0.83 compared to 0.95, and slightly higher for confined splices, 1.00 compared to 0.99 for ACI 408R-03. The respective coefficients of variation for ACI 308 and ACI 408R are 0.19 and 0.10 for unconfined splices and 0.20 and 0.08 for confined splices.

4.0 Analysis of Test Results

The analyses reported in this chapter consider all splitting bond failures for the tests run at KU, NCSU, and UT. Of the 69 test specimens, 64 exhibited splitting bond failures – 31 for unconfined and 33 for confined splices.

4.1 Performance of Development Length Equations

The test and predicted bar stresses at failure for all specimens with unconfined splices are compared in Figure 4.1 and Table 4.1. Table 4.1 shows that both ACI 318-05 [Eq. (3.1)] and ACI 408R-03 [Eq. (3.2)] over predict the splice strength, with test/prediction ratios of 0.87 and 0.98, respectively. Because Eq. (3.1) is meant for use in design and should provide a margin of safety, however, this comparison indicates that ACI 318 is unconservative for development length and splice design for Grade 100 bars. The standard deviation and the range of test/prediction ratios are greater for ACI 318-05 than for ACI 408R-03. The coefficient of variation is 0.20 for ACI 318-05 and 0.11 for ACI 408R-03. The greater accuracy of Eq. (3.2) is evident in Figure 4.1.

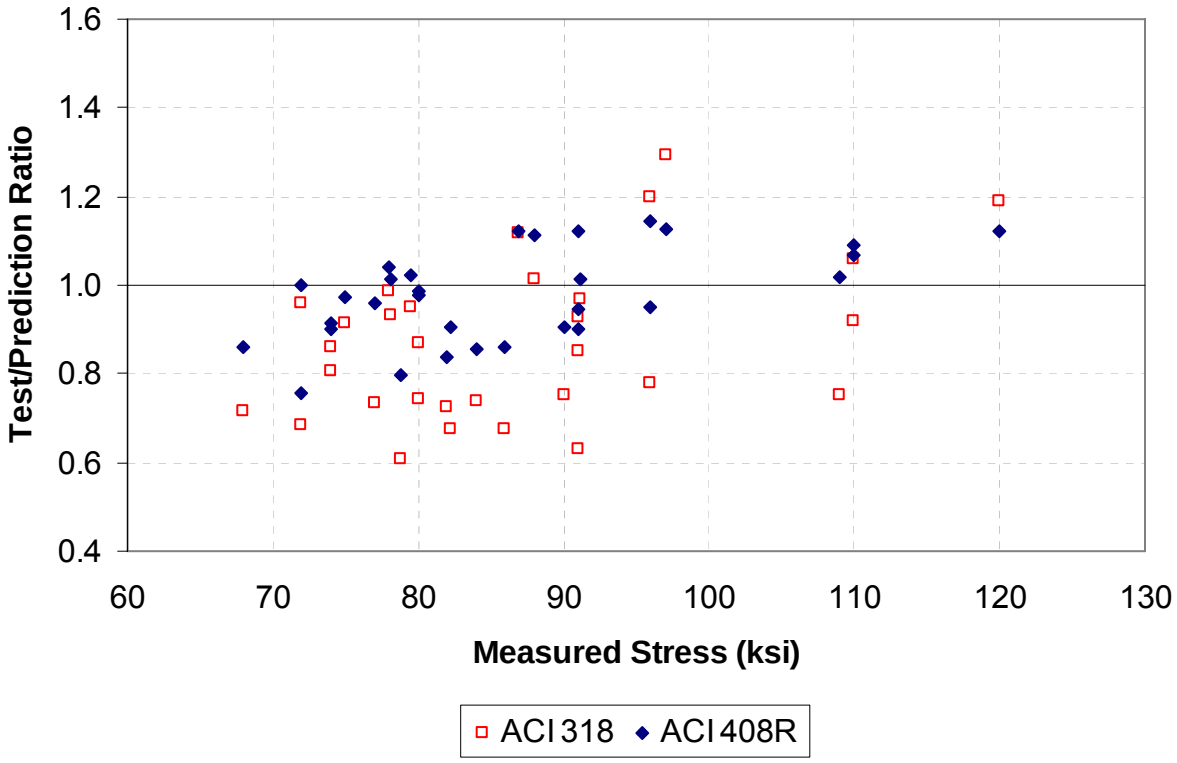

Figure 4.1 – Test/prediction ratios for unconfined beam-splice specimens, all schools

Table 4.1 – Comparison of test and predicted (ACI 318 and 408R) bar stress at failure for unconfined beam-splice specimens, all schools

Specimen	Test	ACI 318-05		ACI 408R-03	
	Stress (ksi)	Stress (ksi)	Test/ Prediction	Stress (ksi)	Test/ Prediction
University of Kansas					
5-5-OC0-3/4	77	105	0.73	80	0.96
5-5-XC0-3/4	82	122	0.68	91	0.91
5-5-OC0-2d_b	87	78	1.12	77	1.12
5-5-XC0-2d_b	91	94	0.97	90	1.01
8-5-OC0-1.5	78	84	0.93	77	1.01
8-5-XC0-1.5	90	120	0.75	99	0.90
8-8-OC0-2.5	79	84	0.95	78	1.02
8-8-XC0-2.5	91	107	0.85	96	0.95
11-8-OC0-2	68	95	0.72	79	0.86
11-8-XC0-2	79	130	0.61	99	0.80
University of Texas					
8-8-OC0-1.5	80	92	0.87	82	0.98
8-8-XC0-1.5	86	127	0.68	100	0.86
8-5-OC0-1.5	74	86	0.86	81	0.91
8-5-XC0-1.5	82	113	0.73	98	0.84
11-5-OC0-3	75	82	0.91	77	0.97
11-5-XC0-3	84	114	0.74	98	0.86
5-5-OC0-3/4	80	108	0.74	81	0.99
5-5-XC0-3/4	91	144	0.63	101	0.90
5-5-OC0-2d_b	88	87	1.01	79	1.11
5-5-XC0-2d_b	110	120	0.92	101	1.09
5-5-OC0-3d_b	97	75	1.29	86	1.13
5-5-XC0-3d_b	120	101	1.19	107	1.12
8-5-SC0-1.5	72	75	0.96	72	1.00
North Carolina State University					
8-5-OC0-2.5	96	80	1.20	84	1.14
8-5-XC0-2.5	110	104	1.06	103	1.07
8-8-OC0-1.5	91	98	0.93	81	1.12
8-8-XC0-1.5	109	145	0.75	107	1.02
11-5-OC0-2	74	92	0.80	82	0.90
11-5-XC0-2	72	105	0.69	95	0.76
11-8-OC0-3	78	79	0.99	75	1.04
11-8-XC0-3	96	123	0.78	101	0.95
			0.87	Average	0.98
			0.18	Std. Dev.	0.11
			0.20	Coef. Var.	0.11
			1.29	Maximum	1.14
			0.61	Minimum	0.76

The comparisons for confined splices are shown in Figure 4.2 and Table 4.2. Both equations underestimate the effect of confinement, with average test/prediction ratios for ACI 318-05 and ACI 408R-03 equal to, respectively, 1.11 and 1.05 (Table 4.2). As observed for unconfined splices, the comparisons for confined splices in Table 4.2 show that the design equation in ACI 318-05 [Eq. (3.1)] results in a higher standard deviation and range of test/prediction ratios than does the equation in ACI 408R [Eq. (3.2)]. The respective coefficients of variation are 0.21 and 0.10 for ACI 318-05 and ACI 408R-03.

Although Eq. (3.2) was calibrated primarily using tests of conventional steel at stresses below 80 ksi and no tests at bar stresses above 120 ksi, the comparisons show it can be used with reasonable accuracy to predict splice strength. ACI 318-05, which is traditionally used for design, however, merits further study for use with Grade 100 steel due to the scatter in the data, and especially the unconservative prediction of bond strength for unconfined splices at high bar stresses.

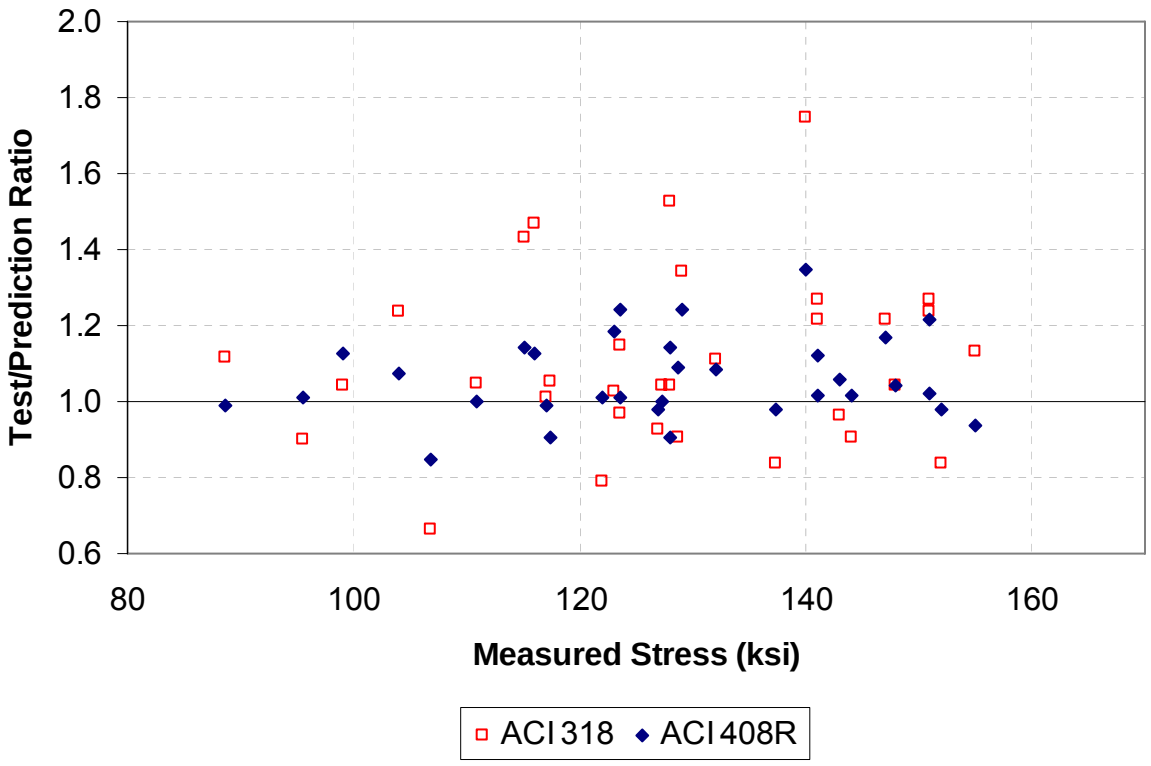

Figure 4.2 – Test/prediction ratios for confined beam-splice specimens, all schools

Table 4.2 – Comparison of test and predicted (ACI 318 and 408R) bar stress at failure for confined beam-splice specimens, all schools

Specimen	Test	ACI 318-05		ACI 408R-03	
	Stress (ksi)	Stress (ksi)	Test/ Prediction	Stress (ksi)	Test/ Prediction
University of Kansas					
8-5-OC1-1.5	124	108	1.15	99	1.24
8-5-XC1-1.5	129	142	0.90	118	1.09
8-5-OC2-1.5	127	122	1.04	127	1.00
8-5-XC2-1.5	143	149	0.96	136	1.06
8-8-OC1-2.5	89	79	1.12	89	0.99
8-8-XC1-2.5	111	106	1.05	111	1.00
8-8-OC2-2.5	115	80	1.43	101	1.14
8-8-XC2-2.5	117	112	1.05	129	0.91
11-8-OC1-2	95	106	0.90	95	1.01
11-8-XC1-2	107	161	0.66	126	0.85
11-8-OC2-2	124	128	0.97	122	1.01
11-8-XC2-2	137	164	0.84	141	0.98
University of Texas					
8-8-OC1-1.5	123	120	1.03	104	1.18
8-8-XC1-1.5	122	155	0.79	121	1.01
8-8-OC2-1.5	147	121	1.21	126	1.17
8-8-XC2-1.5	144	159	0.91	142	1.01
8-5-OC2-1.5	141	111	1.27	126	1.12
8-5-XC2-1.5	148	142	1.04	142	1.04
11-5-OC1-3	104	84	1.24	97	1.07
11-5-XC1-3	117	116	1.01	118	0.99
11-5-OC2-3	128	84	1.52	112	1.14
11-5-XC2-3	141	116	1.22	139	1.01
8-5-SC1-1.5	99	95	1.04	88	1.13
8-5-SC2-1.5	129	96	1.34	104	1.24
North Carolina State University					
8-5-OC1-2.5	140	80	1.75	104	1.35
8-8-OC1-1.5	151	122	1.24	124	1.22
8-8-XC1-1.5	152	182	0.84	155	0.98
11-5-OC1-2	132	119	1.11	122.0	1.08
11-5-OC2-2	151	119	1.27	148.0	1.02
11-5-XC1-2	127	137	0.93	130.0	0.98
11-5-XC2-2	155	137	1.13	165.0	0.94
11-8-OC1-3	116	79	1.47	103.0	1.13
11-8-XC1-3	128	123	1.04	141.0	0.91
			1.11	Average	1.05
			0.23	Std. Dev.	0.11
			0.21	Coef. Var.	0.10
			1.75	Maximum	1.35
			0.66	Minimum	0.85

4.2 NCSU Bond Development Model

An analysis by NCSU (Seliem et al. 2007) of the results for the specimens with unconfined splices using all of the data from the joint research program available at the time provided a useful evaluation of the effect of splice length, concrete cover, and bar size on splice strength.

One of the observations of the NCSU analysis was that, although the ACI 408R equation [Eq. (3.2)] provides an excellent overall match with the test results, as demonstrated in the previous section, the test/prediction ratio drops as the splice length increases, and the decrease is even more pronounced when the data is compared with the provisions of ACI 318 [Eq. (3.1)]. The observations of Seliem et al. (2007) are further supported when the data from all three schools are used, as demonstrated for Eq. (3.2) in Figures 4.3 and 4.4 for unconfined and confined splices, respectively. The downward sloping trend lines in the figures, with slopes of –0.0063 and –0.0030 for unconfined and confined splices, respectively, are obtained using a dummy variable regression analysis (Draper and Smith 1998) based on bar size comparing test/prediction ratios versus ℓ_s/d_b. The trend lines also show that the test/prediction ratios decrease as the bar size increases.

Based on their analysis Seliem et al. (2007) specifically studied the effects of changes in splice length and concrete cover on splice strength, and as a result, proposed the following relationship for the bar stress at splice failure.

$$f_s = \frac{1100\sqrt[4]{f'_c}\sqrt{\ell_s}\sqrt{c}}{d_b} \tag{4.1}$$

where:

f_s = bar stress, psi

f'_c = compressive strength of concrete, psi

ℓ_s = splice development length, in.

d_b = nominal bar diameter, in.

c = minimum value of c_s or c_b, in.

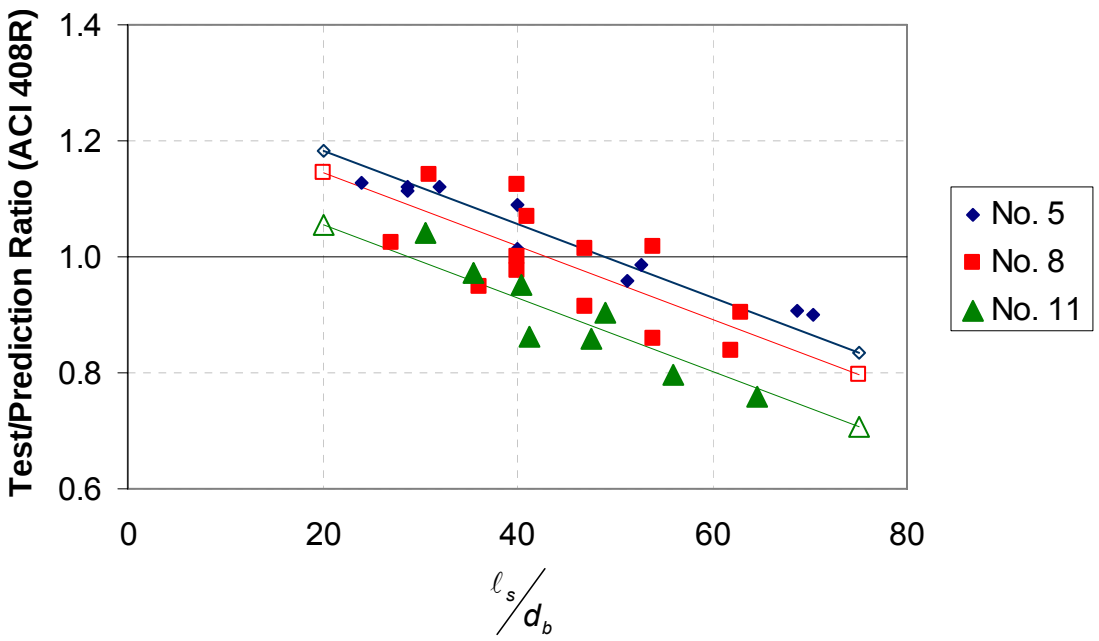

Figure 4.3 – Test/prediction ratios based on ACI 408R [Eq. (3.2)] versus ℓ_s/d_b – unconfined splice data from all schools

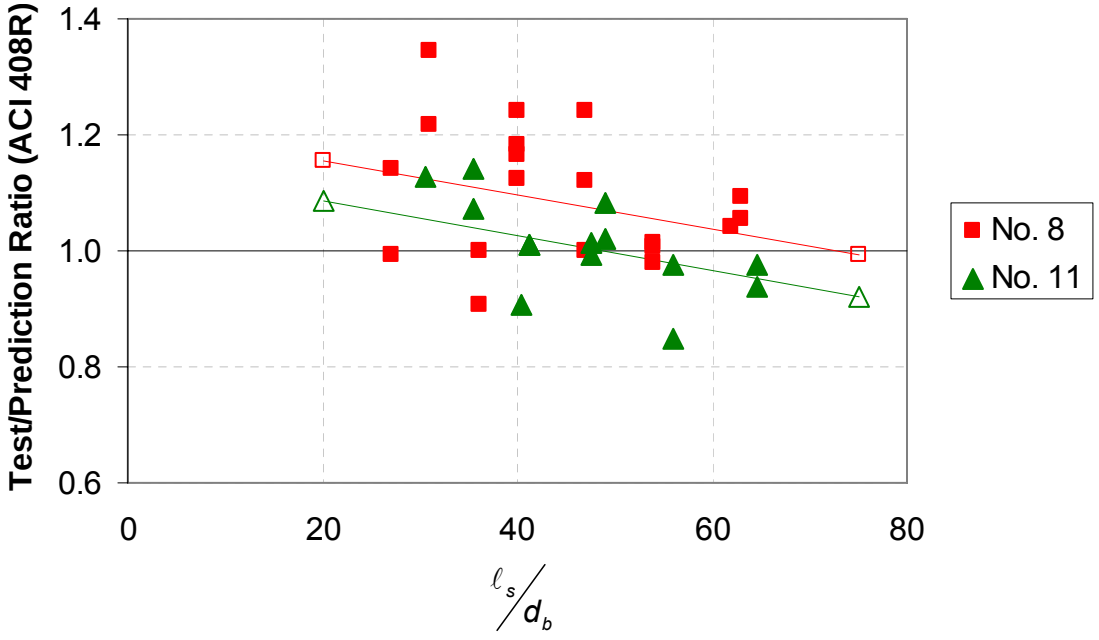

Figure 4.4 – Test/prediction ratios on ACI 408R [Eq. (3.2)] versus ℓ_s/d_b – confined splice data from all schools

c_b = cover of reinforcement being developed, measured to tension face of member, in.

c_s = minimum value of c_{si} or c_{so}, in.

c_{so} = side cover of reinforcing bars, in.

c_{si} = half the clear spacing between reinforcing bars, in.

The test results for the KU, NCSU, and UT specimens with unconfined splices are compared to Eq. (4.1) in Table 4.3. The average test/prediction ratio is 1.06 and the coefficient of variation is 0.13, higher than that obtained using ACI 408R-03 [Eq. (3.2)].

The test/prediction ratios for unconfined splice tests from Table 4.3 are plotted versus ℓ_s/d_b in Figure 4.5. The shallower slope of the dummy variable regression lines shown in this figure (–0.0035) indicate that the NCSU equation may provide a more consistent prediction across a range of ℓ_s/d_b ratios than Eq. (3.2) with a slope of –0.0063.

Equation (4.1) appears to have potential for application in design due to its simplicity, but will require additional study because it was developed based solely on splices designed to produce bar stresses at splice failure of 80 and 100 ksi.

Table 4.3 - Comparison of test and predicted (NCSU) bar stress at failure for unconfined beam-splice specimens, all schools

Specimen	Test	NCSU Proposed	
	Stress (ksi)	Stress (ksi)	Test/ Prediction
University of Kansas			
5-5-OC0-3/4	77	73	1.05
5-5-XC0-3/4	82	77	1.06
5-5-OC0-2d_b	87	66	1.32
5-5-XC0-2d_b	91	72	1.27
8-5-OC0-1.5	78	74	1.05
8-5-XC0-1.5	90	74	1.21
8-8-OC0-2.5	79	83	0.96
8-8-XC0-2.5	91	95	0.96
11-8-OC0-2	68	79	0.86
11-8-XC0-2	79	92	0.86
University of Texas			
8-8-OC0-1.5	80	79	1.02
8-8-XC0-1.5	86	93	0.92
8-5-OC0-1.5	74	76	0.97
8-5-XC0-1.5	82	88	0.93
11-5-OC0-3	75	77	0.97
11-5-XC0-3	84	91	0.93
5-5-OC0-3/4	80	74	1.08
5-5-XC0-3/4	91	86	1.06
5-5-OC0-2d_b	88	71	1.24
5-5-XC0-2d_b	110	84	1.32
5-5-OC0-3d_b	97	84	1.16
5-5-XC0-3d_b	120	97	1.24
8-5-SC0-1.5	72	71	1.01
North Carolina State University			
8-5-OC0-2.5	96	85	1.13
8-5-XC0-2.5	110	97	1.13
8-8-OC0-1.5	91	82	1.12
8-8-XC0-1.5	109	99	1.10
11-5-OC0-2	74	78	0.94
11-5-XC0-2	72	84	0.86
11-8-OC0-3	78	78	1.00
11-8-XC0-3	96	98	0.98
		Average	1.06
		Std. Dev.	0.13
		Coef. Var.	0.13
		Maximum	1.32
		Minimum	0.86

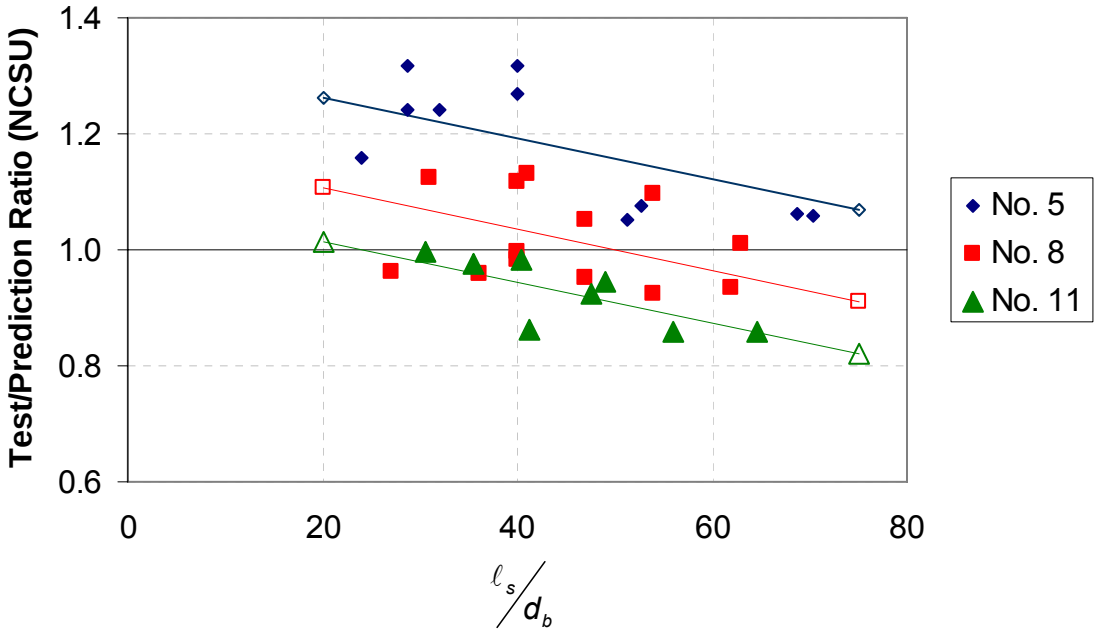

Figure 4.5 – Test/prediction ratios based on NCSU equation [Eq. (4.1)] versus ℓ_s/d_b – unconfined splice data from all schools

5.0 Conclusions and Recommendations

The following conclusions and recommendations are based on the test results and analyses presented in this report.

1. Lap splices using Grade 100 ASTM A 1035 reinforcing steel developed bar stresses up to 143 ksi.
2. At a bar stress of 40 ksi, the maximum flexural crack widths measured at the ends of the splices match or slightly exceed those expected based on earlier crack width criteria. At 67 ksi, however, crack widths are significantly greater than would be expected based on a linear relationship between bar stress and crack width.
3. The development length equation proposed in ACI 408R-03 is an accurate predictor for confined and unconfined bond development for reinforcing steels at bar stresses between 68 and 143 ksi.
4. The development length equation established by ACI 318-05 significantly over predicts bar stress in unconfined splices and under predicts bar stress in confined splices. The latter is appropriate for a design equation; the former is not.
5. The development length equation in ACI 408R-03 resulted in less scatter of test/prediction ratios than ACI 318-05.
6. The use of confining reinforcement significantly increases splice strength and deformation capacity.
7. The bond development equation proposed by NCSU provides an accurate representation of the current test results for unconfined lap splices using Grade 100 ASTM A 1035 reinforcing steel. The limited number of cases considered, however, suggests that additional study is needed before the expression can be recommended for a wider application.

6.0 References

ACI Committee 318, 1999, “Building Code Requirements for Structural Concrete (ACI 318-99) and Commentary (ACI 318R-99),” American Concrete Institute, Farmington Hills, Michigan, 391 pp.

ACI Committee 318, 2005, “Building Code Requirements for Structural Concrete (ACI 318-05) and Commentary (ACI 318R-05),” American Concrete Institute, Farmington Hills, Michigan, 430 pp.

ACI Committee 408, 2001, “Splice and Development Length of High Relative Rib Area Reinforcing Bars in Tension (408.3-01) and Commentary (408.3R-01),“ American Concrete Institute, Farmington Hills, Michigan, 6 pp.

ACI Committee 408, 2003, “Bond and Development of Straight Reinforcing in Tension,“ (ACI 408R-03), American Concrete Institute, Farmington Hills, Michigan, 49 pp.

ASTM A 615/A 615M, 2001, Standard Specification for Deformed and Plain Carbon-Steel Bars for Concrete Reinforcement,” ASTM International, West Conshohocken, PA.

ASTM A 1035/ A 1035M, 2005, Standard Specification for Deformed and Plain, Low-carbon, Chromium, Steel Bars for Concrete Reinforcement,” ASTM International, West Conshohocken, PA.

ASTM C 39/C 39M, 2005, “Standard Test Method for Compressive Strength of Cylindrical Concrete Specimens,” ASTM International, West Conshohocken, PA.

ASTM C172, 2004, “Standard Practice for Sampling Freshly Mixed Concrete.” ASTM International, West Conshohocken, PA.

ASTM C 192/C 192M, 2006, “Standard Practice for Making and Curing Concrete Test Specimens in the Laboratory,” ASTM International, West Conshohocken, PA.

ASTM C 617, 1998, “Standard Practice for Capping Cylindrical Concrete Specimens,” ASTM International, West Conshohocken, PA.

Dawood, M., Seliem, H., Hassan, T., and Rizkalla, S., 2005, “Design Guidelines for Concrete Beams Reinforced with MMFX Microcomposite Reinforcing Bars.” http://www4.ncsu.edu/~srizkal/TechPapers2004/Cairo_2004_design_guidelines_concrete_beams_reinforced_MMFX.pdf.

Draper, N. R. and Smith, H., 1998, *Applied Regression Analysis*, Wiley, New York, 706 pp.

Glass, G., 2007, “Performance of Tension Lap Splices with MMFX High Strength Reinforcing Bars,” Thesis (Master’s), The University of Texas at Austin.

Hognestad, E., 1951, “A Study of Combined Bending and Axial Load in Reinforced Concrete Members,” Bulletin 399, University of Illinois Engineering Experiment Station, Urbana, IL, 128 pp.

Nawy, E., 2003, *Reinforced Concrete, a Fundamental Approach*, Pearson Education, Upper Saddle River, New Jersey, 734 pp.

Seliem, H., Hosny, A., and Rizkalla, S., 2007, “Evaluation of Bond Characteristics of MMFX Steel,” Final Report, North Carolina State University, 71 pp.

Appendix A – Material Properties

Table A.1 – Nominal concrete mix designs

Material	Designation	Mix		Unit
		5 ksi	8 ksi	
Cement	Ashgrove Type I/II; ASTM C 150	564	756	lb
Fine Aggregate, SSD	Kansas River Sand; ASTM C 33/KDOT S-1	1377	1415	lb
Coarse Aggregate, SSD	3/4 in. Crushed Limestone; KDOT LS-3	1823	1635	lb
Water	KDOT Potable	247	242	lb
Water Reducer	W.R. Grace Adva100; ASTM C 494 Type F	0-18	0	oz.
	W.R. Grace AdvaFlex; ASTM C 494 Type F	0	75	oz.
W/C Ratio		0.46	0.32	--
Target Slump		3	5	in.
Compressive Strength		4,670 - 6,050	7,790 - 9,910	psi
Target Age		10	7	days
Actual Age		6-42	4-7	days

*Batch weights reported per CY

Table A.2 – Aggregate properties

Material	Bulk Specific Gravity		Fineness Modulus	Unit Weight	Absorption
	OD	SSD			OD
3/4 in. Crushed Limestone KDOT LS-3	2.48	2.57	--	99 pcf	3.3%
Kansas River Sand; KDOT S-1	2.60	2.62	2.65	--	0.6%

Table A.3 – HRWRA properties

Material	Specific Gravity	Percent Solids
W.R. Grace Adva 100 ASTM C 494 Type F	1.1	30-34%
W.R. Grace AdvaFlex ASTM C 494 Type F	1.0	28-32%

Table A.4 – MMFX Grade 100 reinforcement deformation properties

Bar Size (No.)	Avg. Rib Height (in.)	Avg. Rib Spacing (in.)	Relative Rib Area
5	0.0386	0.415	0.0767
8	0.0644	0.680	0.0838
11	0.0738	0.834	0.0797

Appendix B – Test Result Details

Load Information

Table B.1 – Applied loads, moments, and calculated bar stress for beam-splice tests

Group	Specimen	Endspan to Support Distance	Load/Load Rod				Loading System Weight at Endspan		At Splice Ends					
									Moment from Self Weight		Moment from Applied Loads		Calculated Bar Stress	
			NE	SE	NW	SW	East	West	East	West	East	West	M-Φ	Strength
		(ft.)	(kips)	(kips)	(kips)	(kips)	(kips)	(kips)	(k-ft)	(k-ft)	(k-ft)	(k-ft)	(ksi)	(ksi)
1A	**5-5-OC0-3/4**	4	17.3	17.2	16.8	17.0	0.370	0.384	1.4	1.4	137.8	138.8	77.0	73.9
1B	**5-5-XC0-3/4**	4	18.0	18.5	18.5	18.0	0.370	0.384	1.7	1.7	147.5	147.5	82.2	79.5
2A	**5-5-OC0-2db**	4	8.8	8.9	8.4	8.5	0.370	0.384	1.6	1.6	70.4	71.1	86.9	83.1
2B	**5-5-XC0-2db**	4	8.7	9.8	9.2	9.5	0.370	0.384	1.7	1.7	75.8	75.7	91.2	87.8
3A	**8-5-OC0-1.5**	5.5	23.5	24.5	24.0	24.0	0.370	0.384	3.3	3.3	266.8	267.0	78.1	75.1
	8-5-OC1-1.5	5.5	37.8	38.6	38.5	37.9	0.370	0.384	3.3	3.3	422.3	422.3	123.5	122.1
	8-5-OC2-1.5	5.5	39.5	40.2	40.4	39.6	0.370	0.384	3.3	3.3	440.9	441.6	127.3	125.4
3B	**8-5-XC0-1.5**	5.5	27.6	28.6	27.5	27.6	0.370	0.384	4.0	4.0	306.5	309.8	90.0	87.0
	8-5-XC1-1.5	5.5	39.6	40.3	39.9	39.2	0.370	0.384	3.9	3.9	438.1	440.5	128.7	127.5
	8-5-XC2-1.5	5.5	45.5	46.1	46.1	45.7	0.370	0.384	4.9	4.9	506.7	506.2	143.0	141.4
4A	**8-8-OC0-2.5**	5.5	16.0	16.0	16.1	15.6	0.370	0.384	1.9	1.9	176.7	177.2	79.5	75.9
	8-8-OC1-2.5	5.5	17.0	18.0	18.2	17.8	0.370	0.384	2.0	2.0	197.9	196.7	88.7	85.3
	8-8-OC2-2.5	5.5	22.7	23.4	24.2	22.8	0.370	0.384	1.9	1.9	258.6	257.5	115.0	112.3
4B	**8-8-XC0-2.5**	5.5	18.1	18.3	18.7	17.7	0.370	0.384	2.1	2.1	202.3	202.3	91.1	87.7
	8-8-XC1-2.5	5.5	22.9	22.0	22.3	21.5	0.370	0.384	2.1	2.1	245.4	247.1	111.0	108.1
	8-8-XC2-2.5	5.5	24.1	23.5	23.6	23.2	0.370	0.384	2.1	2.1	262.1	260.7	117.4	114.5
5A	**11-8-OC0-2**	6.5	24.1	23.5	23.6	23.2	0.370	0.384	8.2	8.2	382.2	380.6	67.9	64.5
	11-8-OC1-2	6.5	42.0	42.3	42.3	41.7	0.370	0.384	8.2	8.2	549.0	549.9	95.5	91.7
	11-8-OC2-2	6.5	55.0	50.4	54.3	54.2	0.370	0.384	8.2	8.2	702.5	693.4	123.5	120.3
5B	**11-8-XC0-2**	6.5	33.6	34.3	33.7	34.2	0.370	0.384	9.8	9.8	443.6	443.3	78.9	75.2
	11-8-XC1-2	6.5	45.7	46.5	46.6	45.9	0.370	0.384	9.8	9.8	603.1	601.6	106.9	103.2
	11-8-XC2-2	6.5	60.8	56.2	61.8	61.1	0.370	0.384	11.2	11.2	793.6	770.7	137.3	134.4

Table B.2 – Maximum flexural crack widths at bar stresses bounding 40 and 67 ksi in KU beam-splice tests

Specimen	<40 ksi			>40 ksi			<67 ksi			>67 ksi		
	Total Load	Bar Stress, f_s	Crack Width, w_{cr}	Total Load	Bar Stress, f_s	Crack Width, w_{cr}	Total Load	Bar Stress, f_s	Crack Width, w_{cr}	Total Load	Bar Stress, f_s	Crack Width, w_{cr}
	(kips)	(ksi)	(in.)	(kips)	(ksi)	(in.)	(kips)	(ksi)	(in.)	(kips)	(ksi)	(in.)
5-5-OC0-3/4	32	36.9	0.010	40	45.7	0.013	48	54.5	0.013			
5-5-XC0-3/4	28	32.2	0.010	36	41.5	0.010	52	59.1	0.016	60	67.9	0.016
5-5-OC0-2db	14	37.3	0.010	18	46.9	0.013	22	56.5	0.016			
5-5-XC0-2db	14	36.8	0.010	18	46.3	0.013	26	65.1	0.020	30	74.5	0.020
8-5-OC0-1.5	48	39.8	0.013	56	46.1	0.016	64	52.5	0.020			
8-5-XC0-1.5	48	39.7	0.013	64	52.4	0.016	80	65.0	0.020	88	71.3	0.040
8-5-OC1-1.5	40	33.6	0.013	48	40.0	0.013	80	65.6	0.020			
8-5-XC1-1.5	40	33.7	0.010	56	46.5	0.013	72	59.3	0.040	88	72.0	0.060
8-5-OC2-1.5	48	39.6	0.013	64	52.3	0.016	80	64.9	0.020	88	71.2	0.030
8-5-XC2-1.5	32	27.7	0.010	56	46.2	0.016	80	64.8	0.020	104	83.3	0.020
8-8-OC0-2.5	24	31.1	0.010	32	40.9	0.013						
8-8-XC0-2.5	24	31.4	0.013	32	41.2	0.016	48	60.8	0.020	56	70.6	0.030
8-8-OC1-2.5	30	38.5	0.013	40	50.7	0.020	48	60.5	0.030			
8-8-XC1-2.5	30	38.8	0.013	40	51.1	0.020	48	60.9	0.020	56	70.7	0.030
8-8-OC2-2.5	20	26.2	0.010	32	40.8	0.016	44	55.4	0.020	56	70.0	0.030
8-8-XC2-2.5	*Removed as outlier*			32	41.2	0.010	44	55.9	0.016	56	70.5	0.020
11-8-OC0-2	64	38.1	0.016	*Removed as outlier*								
11-8-XC0-2	64	38.4	0.016	80	47.5	0.020	112	65.5	0.040			
11-8-OC1-2	64	37.6	0.020	*Removed as outlier*			104	59.8	0.050			
11-8-XC1-2	64	39.8	0.013	80	48.9	0.016	96	57.9	0.020	112	67.0	0.050
11-8-OC2-2	64	38.3	0.016	80	47.4	0.020	96	56.4	0.030	120	70.0	0.050
11-8-XC2-2	48	30.5	0.010	80	48.4	0.020	112	66.2	0.030	128	75.1	0.030

Series 1

Both beams in Series 1 contained four No. 5 Grade 100 MMFX longitudinal tension bars. The beams contained a lap splice of length 32 in. (1A) or 43 in. (1B) centered at the midspan of the beam. The total span for Series 1 beams was 15 ft, with an internal span of 7 ft between supports. Series 1 beams were designed with four No. 5 Grade 60 bars as compression reinforcement. Both specimens contained 14 No. 4 closed stirrups spaced at 4 in. in the shear regions beyond the supports. Both specimens had unconfined splices.

The beams in this series were cast with a total depth of 21 in. in the shear regions on either end of the beam and a depth of 20 in. in the central region. The additional depth was added to provide adequate cover around the stirrups which, as designed, had ¼ in. or less clear cover to the tension face. The design cover of ¾ in. was maintained in the test region between supports by placing a 6-ft long, 1-in. thick insert centered at the middle of the beam. The bottom cover was 1 ¾ in. on the longitudinal steel and 1 ¼ in. on the stirrups in the end regions.

The ends of the insert were tapered at a 45º angle to minimize the effect of the stress concentration, although during testing flexural cracks did form at the notch before forming at other sites. The 6-ft length allowed the reduced section to be placed completely between the pin and roller support. In effect, the beams were cast as “dog-bone” sections, with the reduced section covering nearly the entire constant-moment region.

The major impacts of the increased section height in the end spans were a higher precracked section stiffness, the notch’s localizing effect on the initial flexural crack location away from a point directly over the support, and better anchorage for the longitudinal and shear reinforcement in the end spans due to increased cover. Figure B.1, below, shows specimen 5-5-XC0-3/4, with its reduced section.

Cover was maintained within the splice region by suspending the spliced bars from a No. 4 cross bar, placed above the splices, which was then tied to standard 2-in. reinforcing bar chairs protruding up through the splices. Deformations were ground down on the cross bar to reduce its bond to the surrounding concrete and limit any

influence it may have had on splitting crack development. The cross bar was cut to prevent any overhang beyond the outermost bar in the exterior splices. Three chairs were used per cross bar, one between each splice.

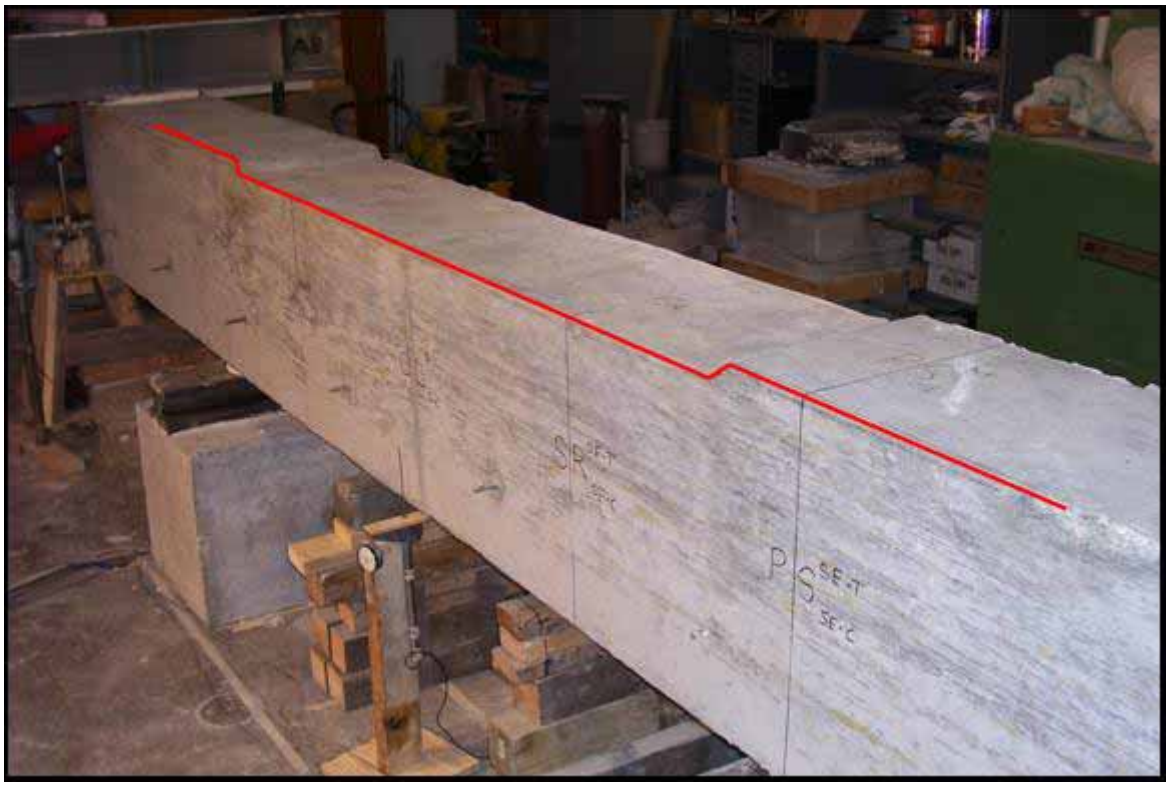

Figure B.1– Specimen 5-5-XC0-3/4 with the reduced "dog-bone" section

The load-deflection behavior of the two beams in Series 1 is shown in Figure B.2, and is quite similar, despite the differences in splice length.

Group 1A

5-5-OC0-3/4

Specimen 5-5-OC0-3/4 failed due to the formation of splitting cracks in the splice region at a bar stress of 77.0 ksi, or 96% of the value predicted by ACI 408R. A photograph of the specimen following the completion of the test is shown in Figure B.3.

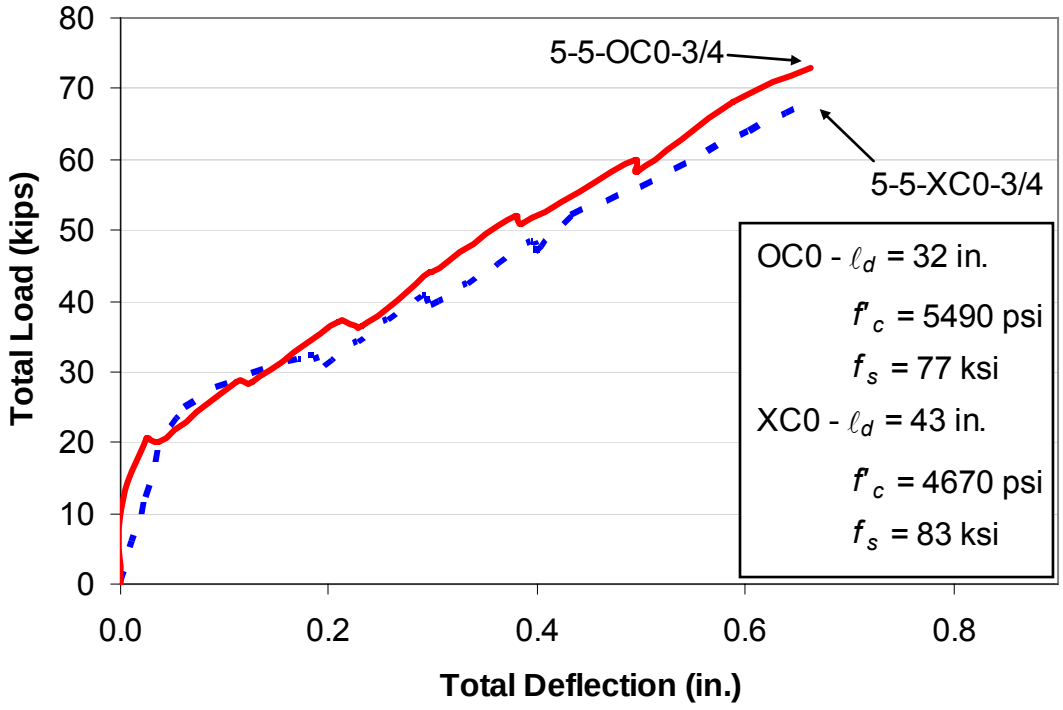

Figure B.2– Load-deflection behavior of Series 1 beams

Figure B.3 – Beam 5-5-OC0-3/4 at the conclusion of the test

Group 1B

5-5-XC0-3/4

Specimen 5-5-XC0-3/4 failed due to the formation of splitting cracks in the splice region at a bar stress of 82.2 ksi, or 91% of the value predicted by ACI 408R. A photograph of the specimen following the completion of the test is shown in Figure B.4

Figure B.4 – Beam 5-5-XC0-3/4 at the conclusion of the test

Series 2

Both beams in Series 2 contained four No. 5 Grade 100 MMFX longitudinal tension bars. Each bar was spliced with a lap length of 18 in. (2A) or 25 in. (2B) centered at the midspan of the beam. The total span for Series 2 beams was 15 ft, with an internal span of 7 ft between supports. Series 2 beams were designed without compression reinforcement, but contained four No. 4 Grade 60 bars to support the upper corners of the shear reinforcement. Both specimens contained fourteen rows of

two No. 4 closed stirrups spaced at 4 in. in each shear region beyond the support, or 28 per end region. Both specimens had unconfined splices.

Series 2 beams were constructed using two separate reinforcement cages in each beam, with each consisting of two tension bars, and two compression bars with their own closed stirrups. This was done to provide shear reinforcement across the entire width of the beam, rather than just at the exterior edges. The two cages were tied together using eight No. 4 bars per specimen.

Because of the 35 in. width of the specimens in Series 2, blockouts were used to reduce the width at the ends of the beam to accommodate the load rods, which were spaced 36 in. apart transversely. 9-in. long by 10-in. tall by 1½-in. deep blockouts were used, reducing the section width to 32 in. at both beam ends over the full height of the specimen. Specimen 5-5-XC0-2d_b used a further 45º transition for the blockout to make the end angled, giving it a total length of 10 ½ in., with 1 ½ in. of transition to the full width.

No chairs or other supports were placed within the splice region for either specimen in Series 2, given the very short splice length. Standard chairs were placed about 4 inches immediately outside of the splice region on both ends of each splice.

The load-deflection curves for the two beams in Series 2 are plotted in Figure B.5.

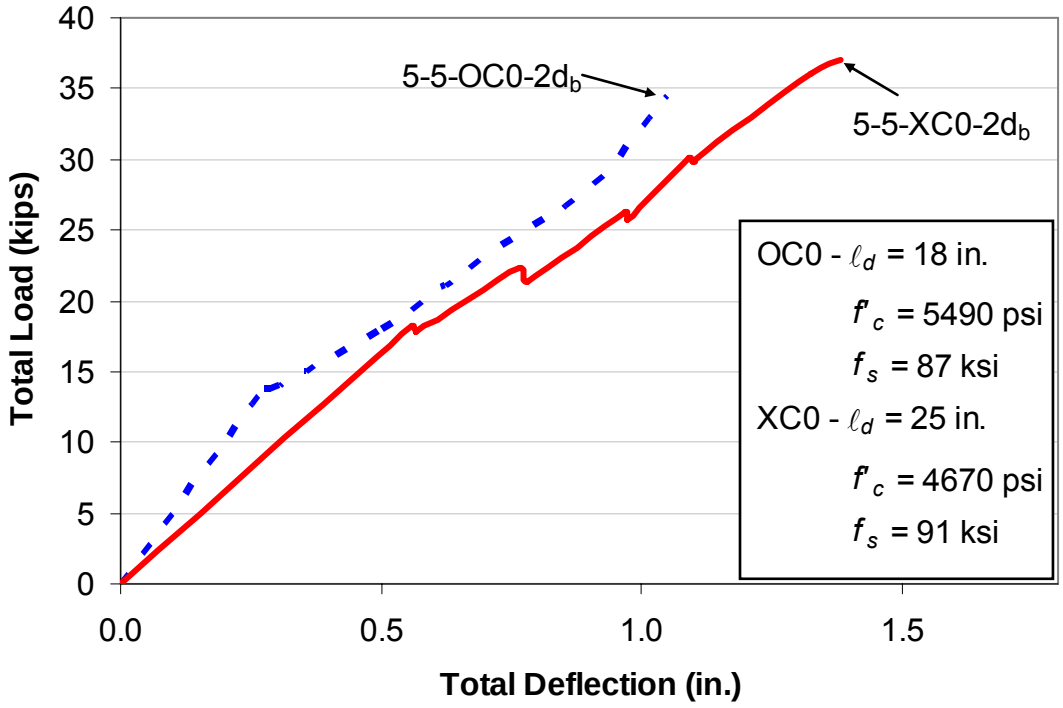

Figure B.5 – Load-deflection behavior of Series 2 beams

During testing on both specimens for Series 2, two distinct “pops” were audibly noted late into the loading, accompanied by small drops in load on the beam. It is believed that these were the exterior splices breaking, although no video or other suitable method exists to verify this. Given that the majority of the load was still being supported, however, loading was continued, and the reported breaking strengths are for the final peak loads on the beam, rather than potential individual splice strengths.

This phenomenon of exterior splices failing prior to failure of the entire specimen was also observed in the tests performed at UT on unconfined No. 5 bar beam-splice specimens, for which Series 1 and Series 2 beams are duplicates. Those conclusions are supported by strain gage data obtained by UT (Glass 2007).

Group 2A

5-5-OC0-2d_b

Specimen 5-5-OC0-2d_b failed due to the formation of bond splitting cracks in the splice region at a bar stress of 86.9 ksi, or 112% of the value predicted by ACI 408R. A photograph of the specimen following the completion of the test is shown in Figure B.6.

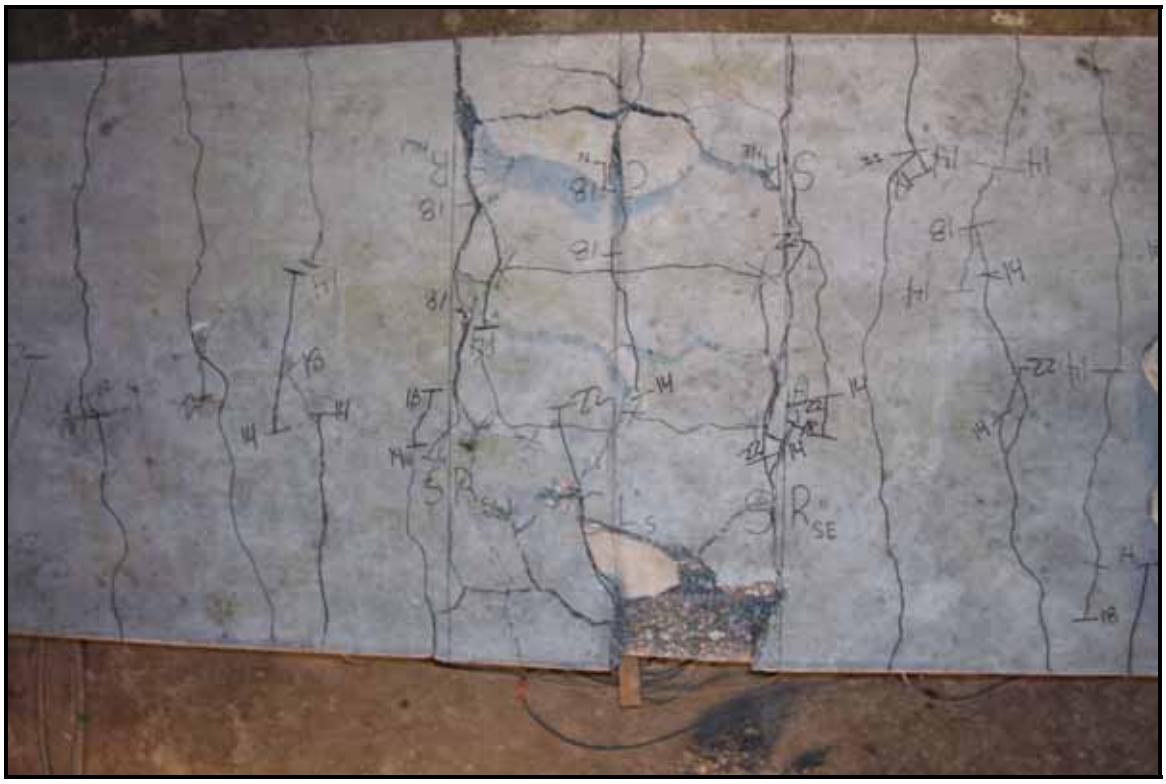

Figure B.6 – Beam 5-5-OC0-2d_b at the conclusion of the test, as viewed from above

Group 2B

5-5-XC0-2d_b

Specimen 5-5-XC0-2d_b failed due to the formation of bond splitting cracks in the splice region at a bar stress of 91.2 ksi, or 101% of the value predicted by ACI 408R. A photograph of the specimen following the completion of the test is shown in Figure B.7.

Figure B.7 – Beam 5-5-XC0-2d_b at the conclusion of the test

Series 3

The beams in Series 3 contained two No. 8 Grade 100 MMFX longitudinal tension bars. The beams contained lap splices with of lengths of 47 in. (4A) or 63 in. (4B) centered at the midspan of the beam. The total span for Series 3 beams was 21 ft, with an internal span of 10 ft between supports. Series 3 beams were designed without compression reinforcement, but contained two No. 4 Grade 60 bars to support the upper corners of the shear reinforcement. Specimen 8-5-XC2-1.5 was an exception because it was cast as a T-beam, as will be described below. All specimens contained 16 No. 4 closed stirrups spaced at 4.5 in. in each shear region beyond the support. The C0 specimens had unconfined splices, while the C1 and C2 specimens contained four and eight No. 4 closed stirrups within the splice region, respectively.

Group 3A

All beams in Group 3A had a splice length of 47 in. The load-deflection behavior is shown in Figure B.8

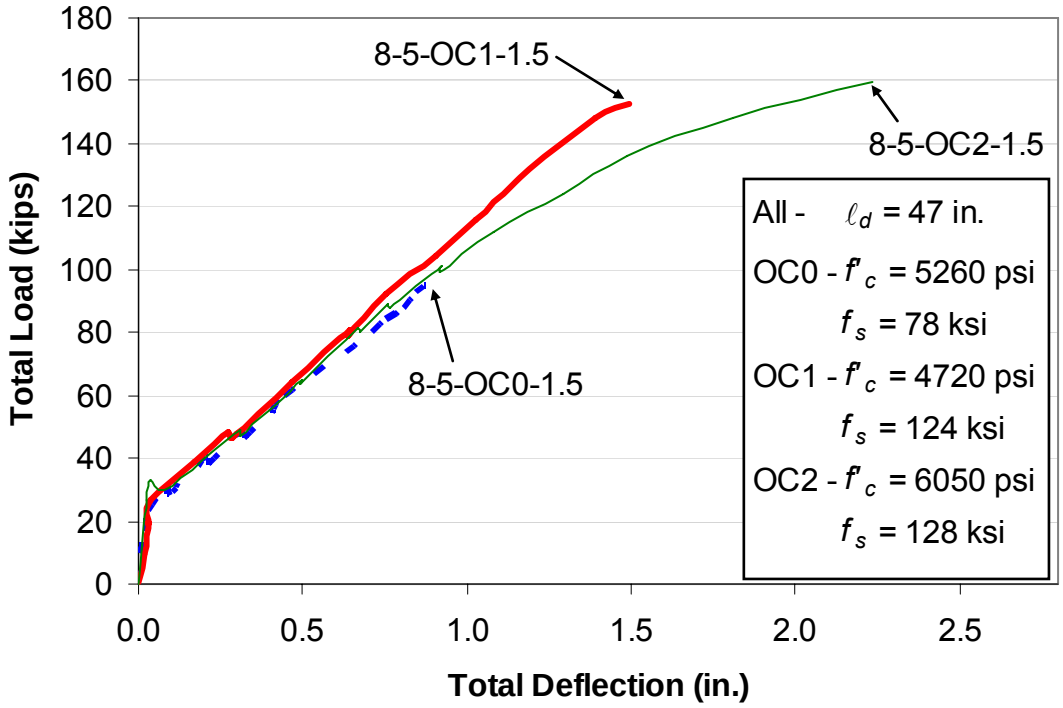

Figure B.8 – Load-deflection behavior of Group 3A beams

8-5-OC0-1.5

Specimen 8-5-OC0-1.5 failed due to the formation of bond splitting cracks in the splice region at a bar stress of 78.1 ksi, or 101% of the value predicted by ACI 408R. A photograph of the specimen following the completion of the test is shown in Figure B.9

Figure B.9 – Beam 8-5-OC0-1.5 at the conclusion of the test

8-5-OC1-1.5

Specimen 8-5-0C1-1.5 failed due to the formation of bond splitting cracks in the splice region at a bar stress of 123.5 ksi, or 124 % of the value predicted by ACI 408R. A photograph of the specimen following the completion of the test is shown in Figure B.10.

Figure B.10 – Beam 8-5-OC1-1.5 at the conclusion of the test

8-5-OC2-1.5

Specimen 8-5-0C2-1.5 failed due to the formation of bond splitting cracks in the splice region at a bar stress of 127.3 ksi, or 100% of the value predicted by ACI 408R. A photograph of the specimen following the completion of the test is shown in Figure B.11.

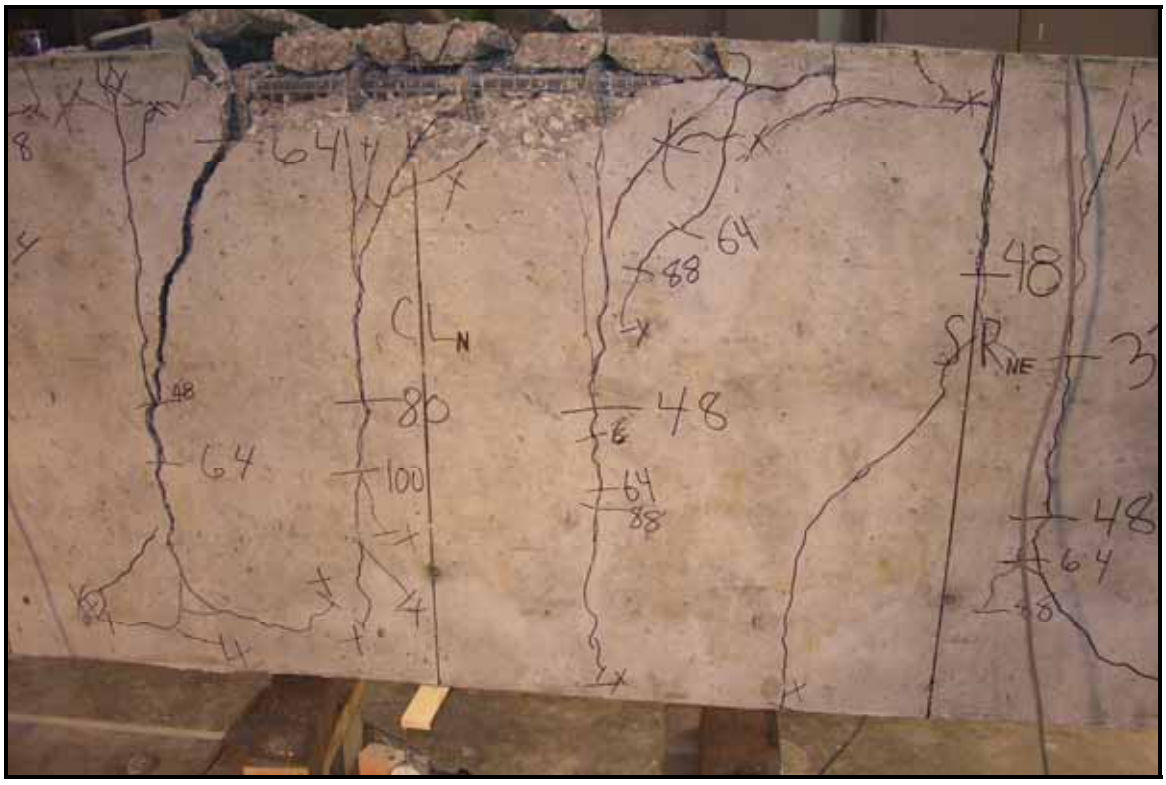

Figure B.11 – Beam 8-5-OC2-1.5 at the conclusion of the test

Group 3B

All beams in Group 3B had a splice length of 63 in. Specimen 8-5-XC2-1.5 was cast as a T-beam with a 28-in. wide, 7-in. deep flange. Specimen 8-5-XC2-1.5 also contained significantly more compression steel than the other beams in the group, 3.16 in.^{2} compared to the 0.40 in.^{2}. As expected, the load-deflection behavior was somewhat stiffer than that of the other two specimens in this group, as shown below in Figure B.12.

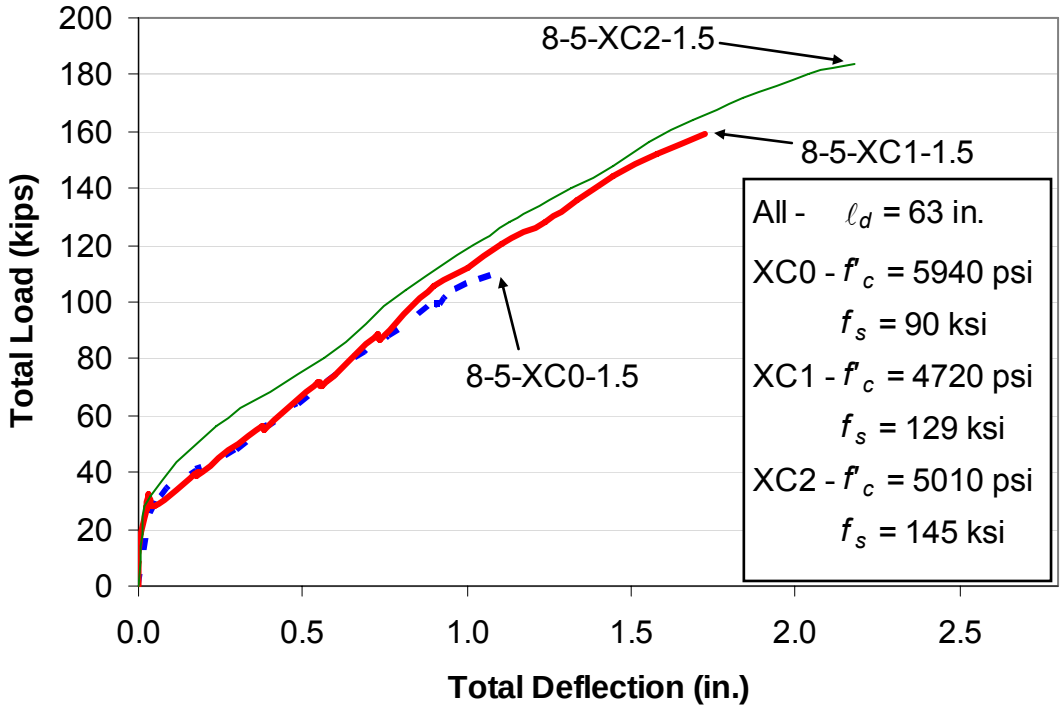

Figure B.12 – Load-deflection behavior of Group 3B beams

8-5-XC0-1.5

Specimen 8-5-XC0-1.5 failed due to the formation of bond splitting cracks in the splice region at a bar stress of 90.0 ksi, or 90% of the value predicted by ACI 408R. A photograph of the specimen following the completion of the test is shown in Figure B.13.

Figure B.13 – Beam 8-5-XC0-1.5 at the conclusion of the test

8-5-XC1-1.5

Specimen 8-5-XC1-1.5 failed due to the formation of bond splitting cracks in the splice region at a bar stress of 128.7 ksi, or 109% of the value predicted by ACI 408R. A photograph of the specimen following the completion of the test is shown in Figure B.14.

Figure B.14 – Beam 8-5-XC1-1.5 at the conclusion of the test

8-5-XC2-1.5

Specimen 8-5-XC2-1.5 failed by splitting in the splice region at a bar stress of 143.0 ksi, or 106% of the value predicted by ACI 408R. Only one splice appeared to have spalled the concrete, but upon failure of this splice, the beam lost approximately half the load it was carrying. It was later apparent that wooden blocks placed beneath the ends of the beam to prevent the ends from falling to the floor after failure were stacked high enough to prevent the second splice from failing. The test was discontinued at this point. A photograph of the specimen following the completion of the test is shown in Figure B.15.

Figure B.15 – Beam 8-5-XC1-1.5 at the conclusion of the test

In addition to being cast as a T-beam, specimen 8-5-XC2-1.5 differed from other beams in this program in that it contained U-stirrups with seismic hooks in the shear regions outside of the supports rather than the closed stirrups used in all other beams. U-stirrups were chosen to conserve material given that specimen 8-5-XC2-1.5 was a duplicate of a previously cast beam that failed in flexure. Closed stirrups were used, as normal, in the splice region for confinement.

The U-stirrups were closed with opposing U-stirrups that extended into the flanges to support two of the four No. 8 Grade 60 bars used as compression reinforcement. The other two No. 8 bars were placed within the hooks on the primary U-stirrups that confined the longitudinal steel in the ends. Two No. 3 bars were cast into specimen 8-5-XC2-1.5 at a depth of 5 ¼ in. from the top of the flange to anchor the hooks of the upper U-stirrups, but were not considered in the analysis of the beam for either tension and compression.

Series 4

All beams in Series 4 contained two No. 8 Grade 100 MMFX longitudinal tension bars. The beams had a lap splice of length 27 in. (4A) or 36 in. (4B) centered at the midspan of the beam. The total span for Series 5 beams was 21 ft with an internal span of 10 ft between supports. Series 4 beams contained two No. 8 Grade 60 bars as compression reinforcement. All specimens contained 15 closed stirrups spaced at 5 in. in each shear region beyond the support. C0 specimens had unconfined splices, while C1 and C2 specimens contained 2 and 5 No. 4 closed stirrups, respectively.

Group 4A

All beams in Group 4A had a splice length of 27 in. The load-deflection behavior is shown in Figure B.16

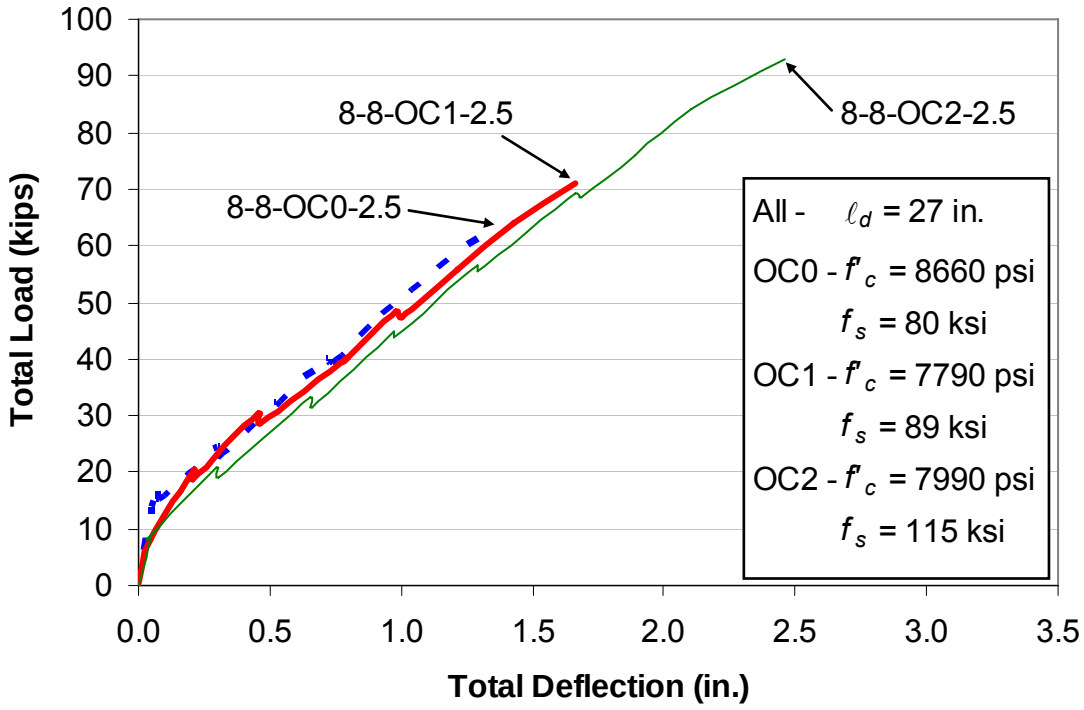

Figure B.16 – Load-deflection behavior of Group 4A beams

8-8-OC0-2.5

Specimen 8-8-OC0-2.5 failed due to the formation of bond splitting cracks in the splice region at a bar stress of 79.5 ksi, or 102% of the value predicted by ACI 408R. A photograph of the specimen following the completion of the test is shown in Figure B.17.

Figure B.17– Beam 8-8-OC0-2.5 at the conclusion of the test

8-8-OC1-2.5

Specimen 8-8-OC1-2.5 failed due to the formation of bond splitting cracks in the splice region at a bar stress of 88.7 ksi, or 99% of the value predicted by ACI 408R. A photograph of the specimen following the completion of the test is shown in Figure B.18.

Figure B.18 – Beam 8-8-OC1-2.5 at the conclusion of the test

8-8-OC2-2.5

Specimen 8-8-OC2-2.5 failed due to the formation of bond splitting cracks in the splice region at a bar stress of 115.0 ksi, or 114% of the value predicted by ACI 408R. A photograph of the specimen following the completion of the test is shown in Figure B.19.

Figure B.19 – Beam 8-8-OC2-2.5 at the conclusion of the test

Group 4B

All beams in Group 4B had a splice length of 36 in. The load-deflection behavior is shown in Figure B.20.

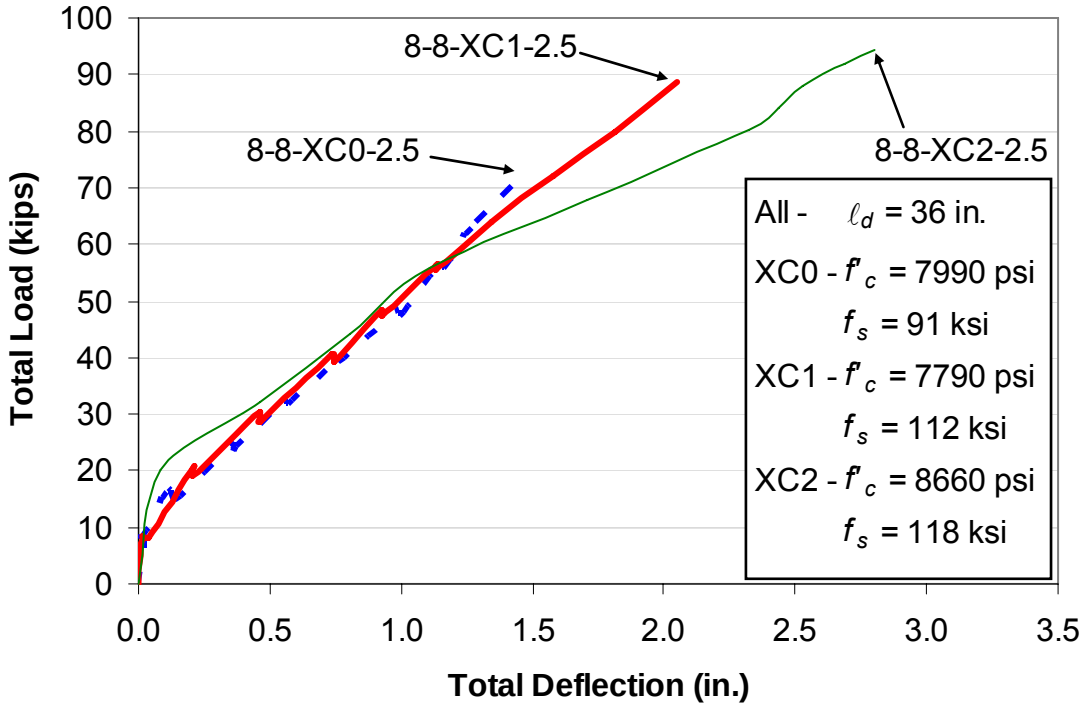

Figure B.20 – Load-deflection behavior of Group 4B beams

8-8-XC0-2.5

Specimen 8-8-XC0-2.5 failed due to the formation of bond splitting cracks in the splice region at a bar stress of 91.1 ksi, or 95% of the value predicted by ACI 408R. A photograph of the specimen following the completion of the test is shown in Figure B.21.

Figure B.21 – Beam 8-8-XC0-2.5 at the conclusion of the test

8-8-XC1-2.5

Specimen 8-8-XC1-2.5 failed due to the formation of bond splitting cracks in the splice region at a bar stress of 111.0 ksi, or 100% of the value predicted by ACI 408R. A photograph of the specimen following the completion of the test is shown in Figure B.22.

Figure B.22 – Beam 8-8-XC1-2.5 at the conclusion of the test

8-8-XC2-2.5

Specimen 8-8-XC2-2.5 failed due to the formation of bond splitting cracks in the splice region at a bar stress of 117.4 ksi, or 91% of the value predicted by ACI 408R. A photograph of the specimen following the completion of the test is shown in Figure B.23.

Figure B.23 – Beam 8-8-XC2-2.5 at the conclusion of the test

Specimen 8-8-XC2-2.5 was the sole specimen with a nominal target bar stress of 140 ksi that was not cast as a T-beam. Due to the first duplicate of specimen 8-5-XC2-1.5 experiencing a flexural failure at a bar stress near 140 ksi after the casting of this specimen, external stirrups were used in an attempt to confine the concrete at the highest moment regions away from the test region. Each external stirrup consisted of one C6x8.2 channel on both the top and bottom of the beam connected with ½-in. all-thread rod on each side of the beam. Four stirrups were used sequentially on each side of the splice region beginning at the edge of the bearing plate for the support and terminating roughly 10 in. from the end of the splice region. The bearing faces of the channels were attached with Hydrostone to the beam. A photograph showing these stirrups is shown in Figure B.24. The weight of the external stirrups was not included in the applied loads for moment calculation.

Figure B.24 – External stirrups used on beam 8-8-XC2-2.5

Series 5

All beams in Series 5 contained two No. 11 Grade 100 MMFX longitudinal tension bars. The beams had a lap splice of length 58 in. (5A) or 79 in. (5B) centered at the midspan of the beam. The total span for Series 5 beams was 24 ft with an internal span of 11 ft between supports. Series 5 beams were designed without compression reinforcement, but contained two No. 4 Grade 60 bars to support the upper corners of the shear reinforcement. Specimen 11-8-XC2-2, a T-beam, is an exception, as described below. All specimens contained 19 No. 5 closed stirrups spaced at 4.5 in. in each shear region beyond the support. The C0 specimens had unconfined splices, while the C1 and C2 specimens contained four and nine No. 4 closed stirrups, respectively.

Group 5A

All beams in Group 5A had a splice length of 58 in. The load-deflection behavior is shown below in Figure B.25

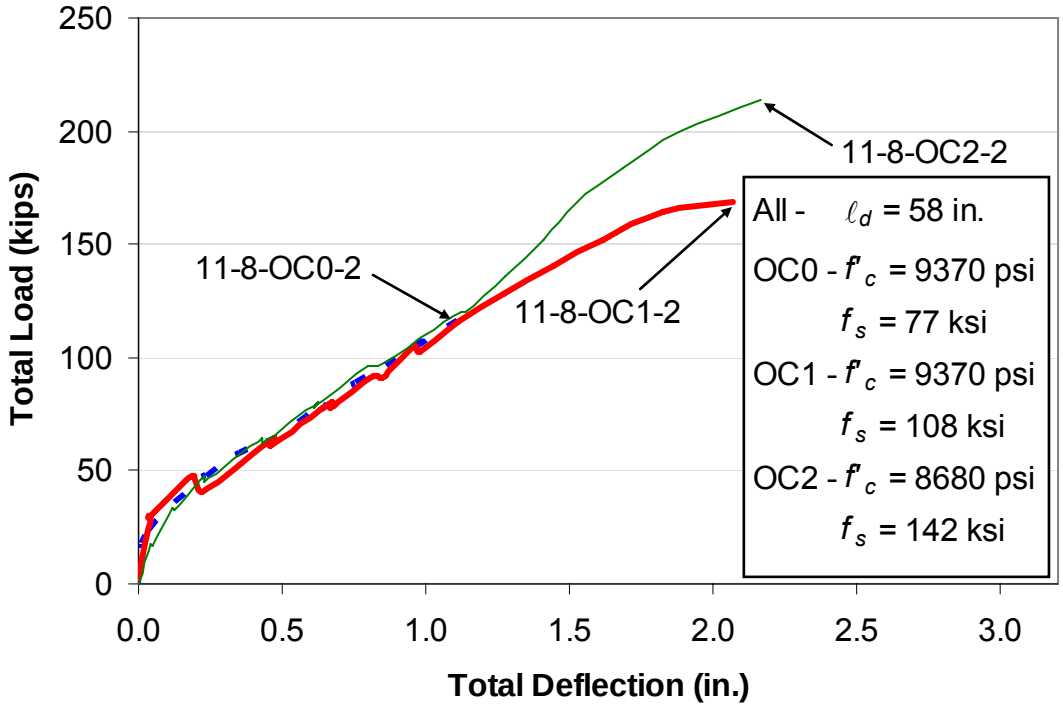

Figure B.25 – Load-deflection behavior of Group 5A beams

11-8-OC0-2

Specimen 11-8-OC0-2 failed due to the formation of bond splitting cracks in the splice region at a bar stress of 67.9 ksi, or 86% of the value predicted by ACI 408R. A photograph of the specimen following the completion of the test is shown in Figure B.26.

Figure B.26 – Beam 11-8-OC0-2 at the conclusion of the test

11-8-OC1-2

Specimen 11-8-OC1-2 failed due to the formation of bond splitting cracks in the splice region at a bar stress of 95.5 ksi, or 101% of the value predicted by ACI 408R. A photograph of the specimen following the completion of the test is shown in Figure B.27.

Figure B.27 – Beam 11-8-OC1-2 at the conclusion of the test, as viewed from above

11-8-OC2-2

Specimen 11-8-OC2-2 failed due to the formation of bond splitting cracks in the splice region at a bar stress of 123.5 ksi, or 101% of the value predicted by ACI 408R. A photograph of the specimen following the completion of the test is shown in Figure B.28.

Figure B.28 – Beam 11-8-OC2-2 at the conclusion of the test

Beam 11-8-OC2-2 was loaded to approximately 48 kips total load, at which point it was noted that the load distribution across the four load rods was uneven compared to that typically observed during tests. Additionally, at that load step, a severe and continual reduction in load was noted. As such, although the beam was well beyond the cracking load, all load was removed from the beam and the hydraulic system was completely reset and tightened. The beam was then reloaded from zero, and stable results were obtained for the remainder of the test.

Group 5B

All beams in Group 5B had a splice length of 79 in. Specimen 11-8-XC2-2 was cast as a T-beam with a 38-in. wide, 7-in. deep flange. Specimen 11-8-XC2-2 was also cast with significantly more compression steel, 3.56 in.^{2} compared with the 0.40 in.^{2} found in the other beams in the group. The load-deflection behavior is somewhat stiffer for the T-beam compared to the other two specimens in the group, as shown in Figure B.29.

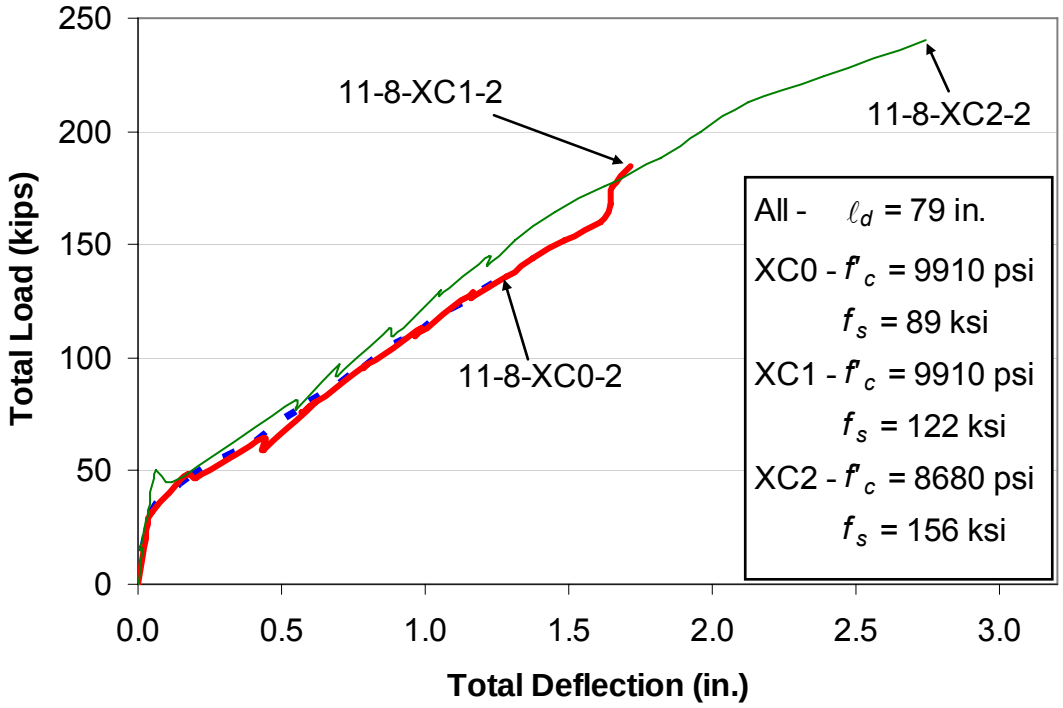

Figure B.29 – Load-deflection behavior of Group 5B beams

11-8-XC0-2

Specimen 11-8-XC0-2 failed due to the formation of bond splitting cracks in the splice region at a bar stress of 78.9 ksi, or 80% of the value predicted by ACI 408R. A photograph of the specimen following the completion of the test is shown in Figure B.30.

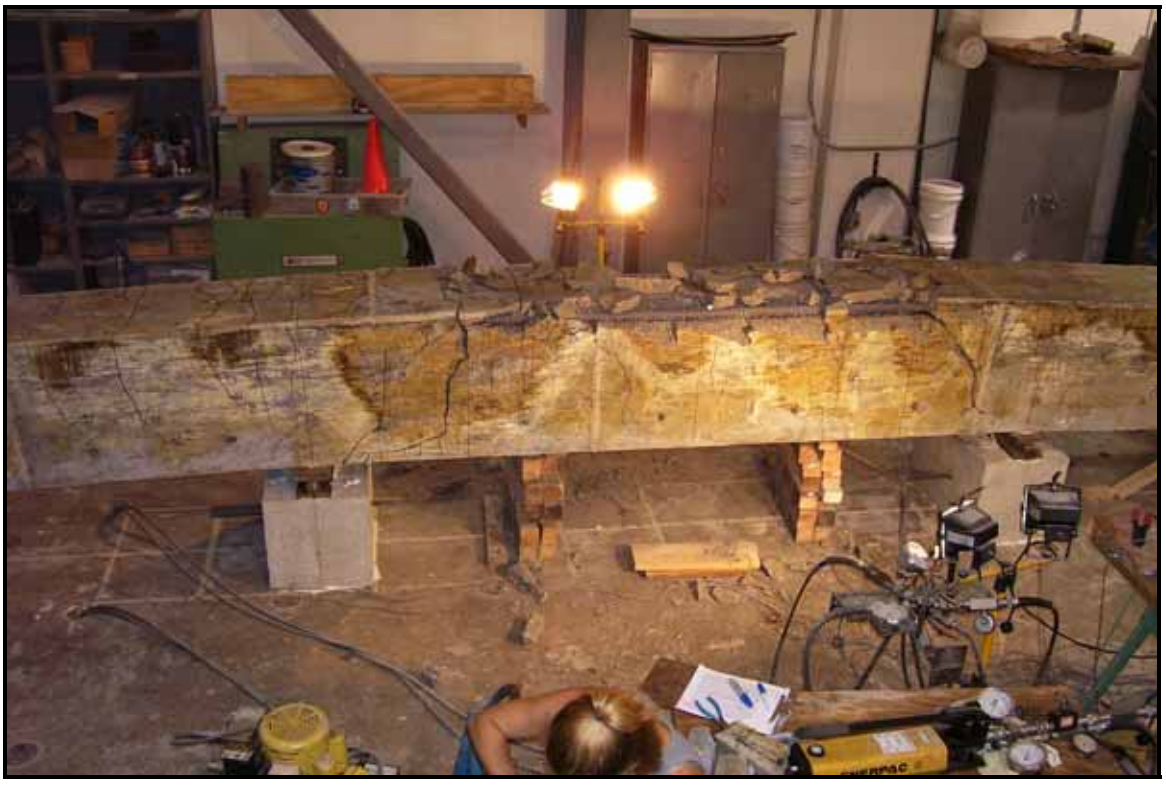

Figure B.30 – Beam 11-8-XC0-2 at the conclusion of the test

11-8-XC1-2

Specimen 11-8-XC1-2 failed due to the formation of bond splitting cracks in the splice region at a bar stress of 106.9 ksi, or 85% of the value predicted by ACI 408R. A photograph of the specimen following the completion of the test is shown in Figure B.31.

Figure B.31 – Beam 11-8-XC1-2 at the conclusion of the test

11-8-XC2-2

Specimen 11-8-XC2-2 failed due to the formation of bond splitting cracks in the splice region at a bar stress of 137.3 ksi, or 98% of the value predicted by ACI 408R. A photograph of the specimen following the completion of the test is shown in Figure B.32.

Figure B.32 – Beam 11-8-XC2-2 at the conclusion of the test

Given the 38-in. flange width of specimen 11-8-XC2-2, blockouts were used to reduce the flange width at the ends of the beam to accommodate the load rods, which were spaced 36 in. apart transversely. 9-in. long by 7-in. tall by 4-in. deep block-outs were used to eliminate a portion of the final nine inches of the flange, resulting in a final reduced flange width at both ends of approximately 30 in.